Route exploration of valorization of buckwheat waste based on subcritical liquid treatment
(亜臨界液体処理によるソバ廃材の付加価値化方法に関する検討)

Hokkaido University　Graduate School of Agriculture

Frontiers in Production Sciences　Doctor Course

Yuan Yongheng

Abstract

Buckwheat waste (BWW), which includes husks, leaves, and straw, is usually thrown away or burned. This leads to serious pollution problems and a waste of resources. BWW is rich in cellulose, hemicellulose, antioxidants, and various sugars; thus, it can be considered as a potential source to improve the economic benefits of buckwheat cultivation. However, components such as sugars and antioxidants in BWW are often cross-linked with structural compounds via chemical bonds. Therefore, it is vital to develop a strategy to facilitate depolymerization of these structures and improve the utilization efficiency of BWW.

In this study, subcritical water has been developed to improve the yields of saccharides from BWW. Subcritical ethanol solution was used to increase the yields of bioactives components. The scale-up to an industrial level was tested on a pilot scale. The hydrolysate prepared from subcritical seawater treatment of BWW has also been tested as a liquid fertilizer to promote lettuce growth.

1. Subcritical water treatment of BWW for sugar extraction

A subcritical water treatment (SWT) was chosen for cellulose and hemicellulose degradation to produce saccharides from raw BWW. The sum of saccharides yields in the liquid sample were compared. A higher sum of saccharides yields of 4.10 % was obtained at a relatively lower severity factor of 3.24. The contents of cellulose, hemicellulose, and lignin were analyzed in the residue after SWT. The result shows that lignin was dominant in the residue. The irregular pores were observed by SEM after SWT due to the removal of some hemicellulose, and lignin. Finally, an overall mass conversion based on saccharides production was carried out. The result reflects a considerable yield of saccharides from BWW by SWT.

2. BWW depolymerization using a subcritical ethanol solution for extraction of bioactive components: from the laboratory to pilot scale

Subcritical ethanol solution treatment (SEST) was used to depolymerize BWW and extract bioactive components such as phenolics, flavonoids, and sugars on both the laboratory and the pilot scale. On the laboratory scale, various treatment conditions were compared. Depolymerization of the microstructure was evaluated by the detection of solid components, and the extraction of bioactive compounds was studied by the detection of liquid components. The mechanism of SEST depolymerization of BWW and the extraction of bioactive components is discussed. Scaling up to an industrial level was tested on a pilot scale, and solid and liquid

components were identified. The total phenolics content increased significantly because SEST promoted the degradation of lignin and the solubilization of extractive components. The yield of total flavonoids did not change significantly with increases in the temperature, which could be attributed to the degradation of some flavonoid components at high temperature. Reducing sugars were present mainly in the form of polysaccharides, which was attributed to the low temperature. The maximum total yields of phenolics, flavonoids, and reducing sugars were 29.8 ± 0.1, 13.9 ± 0.5 and 33.9 ± 0.5 g/kg, respectively. This study provides valuable reference data for BWW utilization on a pilot scale.

3. Effect of hydrolysate from subcritical seawater treatment of BWW as liquid fertilizer on lettuce growth

BWW was treated with subcritical seawater treatment (SST) at different treatment temperatures. The collected hydrolysate was used as a liquid fertilizer for lettuce growth, and finally the physico-chemical properties of hydrolysate and the growth indexes of lettuce under each condition were examined. The results showed that after SST of BWW, the salt content decreased while some antioxidants and sugars increased because of the hydrolysate. The hydrolysate was able to promote the growth of lettuce. The maximum weight of lettuce cultivated with the hydrolysate was 22 g, with an average height of 14 cm at 170 ℃ of SST. This study combined the reuse of biomass and seawater for agricultural cultivation, which provided a new way to use BWW, it acts as a reference for the irrigation of seawater in agricultural cultivation, and also increased the added value of buckwheat cultivation.

Acknowledgement

The prime years won't return

, a morning is hard to come by again. Seize the opportunity and motivate oneself, as time waits for no one. The three years of studying abroad have passed in the blink of an eye. During my time in Japan, I have received assistance from many people in my studies and daily life. I would like to express my heartfelt gratitude to them.

Firstly, I would like to express my gratitude to Japan, this beautiful country, and its people. I have spent a precious and unforgettable time here, which has had a profound impact on my personal and professional life. The people of Japan are full of warmth and friendliness. During my study abroad experience in Japan, I had the opportunity to interact, collaborate, and learn from people from around the world. This international environment has broadened my horizons and cultivated my abilities in cross-cultural communication and collaboration. I am also fortunate to have participated in the development and progress of your country, which is a valuable experience in my life. I will always cherish the time and all the experiences I had here.

Secondly, I would like to express my gratitude to my advisor, Associate Professor Naoto Shimizu. Professor Shimizu is knowledgeable, meticulous, kind-hearted, and always willing to help. From topic selection, conceptualization, experimentation, to writing the paper, I have received Professor Shimizu's careful guidance and selfless assistance. Professor Shimizu frequently communicates with me to understand my research and personal circumstances. Additionally, Professor Shimizu is genuinely concerned about my well-being and has shown me tremendous care, understanding, and support. I hold profound respect and heartfelt gratitude towards Professor Shimizu.

Thirdly, I would like to express my gratitude to Hokkaido University and the Faculty of Agriculture, as well as the leaders and staff members. The various resources and support provided by the university, including the library, laboratories, research centers, and other academic facilities, have laid a solid foundation for my learning and research. The university staff have put in a lot of effort to create an

excellent learning environment and provide high-quality education. They have also offered me guidance and support, helping me to adapt to the academic and life challenges smoothly.

Fourthly, I would like to express my gratitude to the Japan government, SDGs scholarship and the staff involved. Thank you for providing me with these valuable scholarships opportunities. These scholarships not only offers me financial assistance but also recognizes my dedication to learning and striving for excellence. These scholarships will allow me to focus on my studies and pursue my academic dreams. I would also like to thank the judges and members of the scholarship committee for their hard work and fair evaluation, which ensured the smooth implementation of this scholarship program. I sincerely thank you all and hold deep respect for your contributions.

Fifth, I would like to express my sincere gratitude and deep respect to Professor Kazunori Iwabuchi and Professor Hideyuki Matsuura, the reviewers of my graduation thesis. I am aware of the substantial time and effort you have dedicated to carefully reviewing my paper and providing valuable feedback and suggestions, which have been an immense support and help to me. I wholeheartedly appreciate your willingness to take on this task, as your expertise and experience have added immense value to my thesis. I will forever be grateful for your assistance and support.

Sixth, I would like to express my gratitude to every member of the research group. The senior students have provided me with guidance and assistance, while the junior students have supported and helped me during my experimental process. The mutual support and care among classmates of the same year throughout these three years are greatly appreciated.

Seventh, Thank you to my hardworking parents who have always been the driving force and support in my life journey. I am grateful for your unwavering dedication. I will continue to strive forward and become an outstanding individual.

Finally, I would like to express my gratitude once again to everyone who has helped and cared for me. May you all have good health, successful careers, and eternal happiness!

Contents

List of figures

List of tables

Chapter 1. Introduction

1.1 World energy resource shortage

For the development of the human society, most of fossil fuels was used from many years ago, and the bad influence has highlight in the industrial revolution due to large scale utilization of the fossil fuels. Nowadays, the energy consumption has increased faster and the problems of global warming has become increasingly serious due to the consumption of fossil fuels. But energy is the bases for human survive, thus more and more countries has bring a scheme to deal with the challenges (Bahram et al., 2021; Wang et al., 2016). It's essential and emergency to explore and realize the transitions from the fossil fuels to renewable energy for low-carbonizing the world economy, alleviating global climate change and energy issues (Levenda et al., 2021; Wu et al., 2021). A lot of renewable energy has been considered by researchers, such as wind power and solar irradiance, but it's intermittent and periodically variable, so the capacity factors units are lower than fossil fuel units significantly (Michaelides et al., 2020).

1.2 Biomass energy resources

As the fourth largest energy resource, next to coal, oil and natural gas, lignocellulose biomass energy play a significant role in the whole energy system. In general, lignocellulosic biomass can be broadly classifified into virgin biomass, which includes all naturally occurring terrestrial plants such as trees, bushes and grass, waste biomass from various industrial sectors such as agricultural and forestry, and energy crop with high yield of lignocellulosic biomass produced to serve as a raw material for production of biofuel, examples include switch grass and Elephant grass (Ren et al., 2016). Lignocellulosic biomass dominate by cellulose, hemicellulose and lignin, as the most abundant renewable biomass resource, has been focused due to it's utilization of low value, carbon-neutral, availability (Ren et al., 2016). As one of the most important lignocellulose biomass, waste biomass such as, corn stover, woods and even tea waste and so on has been applied a lot in ferment sugar, enzymatic hydrolysis, biogas and other biofuel's production by various methods, to realized the resource utilization (Chen et al., 2021; Zeng et al., 2021; Sabzoi et al., 2017;

Mohammed et al., 2020; Rajapaksha et al., 2020; Suely et al., 2020).

1.3 Buckwheat

Buckwheat is one of the ancient crops originated from China and broadly cultivated in the world, and production was more than 2.90 million tons in 2018 (Nurul Huda et al., 2021). It is categorized as a pseudo cereal, which shows both differences and similarities with cereals. It has been grown and used for food or medicine, because of the balanced amino-acid composition of its proteins, and its content of fiber, resistant starch, trace elements, vitamins and antioxidants (Holasova et al., 2002; Bonafaccia et al., 2003; Ji et al., 2019). Having a lot of research was focused on the edible (seed) part of the buckwheat, due to these riching nutrients component and elements (Nurul Huda et al., 2021).

Buckwheat waste (BWW) is the residue left after harvesting the fruits. It is the most important part of buckwheat, including husk, leaves and straw. It has been neglected, and abandoned or combustion. It's makes serious pollution and waste of resource. While the BWW also richness in cellulose, hemicellulose, antioxidants and various sugar has been reported (Nurul Huda et al., 2021; Milica et al., 2021; Dziedzic et al., 2018). So it's is considered a potential source that may be used to improve the conversion rate and economic benefits of buckwheat cultivation.

1.4 The composition of BWW

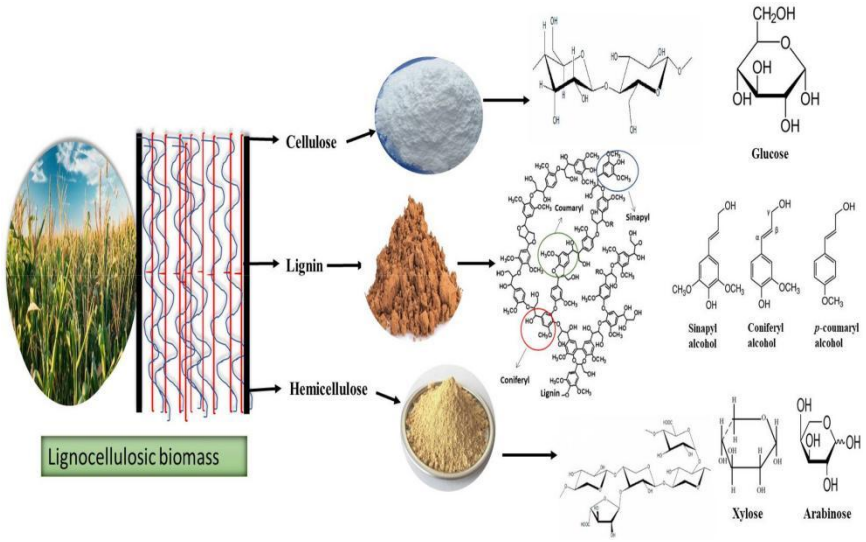

Figure 1.1 The structure of lignocellulose biomass (Sharma et al., 2023).

1.4.1 Cellulose

Cellulose which made up of glucose is the most abundant organic substance in the world. Commonly, the cellulose is insoluble in water and organic solvents, as well as in dilute alkaline solutions due to the presence of hydrogen bonds between molecules, but readily hydrolysable under acidic conditions. Under certain conditions, cellulose can be decomposed into glucose by reaction with water.

1.4.2 Hemicellulose

Hemicellulose consists of hexose, mannose, galactose, pentose, xylose (a five-carbon aldose) and arabinose. It is hydrophilic, soluble in alkali and more easily hydrolysed than cellulose in the presence of acid. Under certain conditions, hemicellulose mainly undergoes interchain breakage and the product is mainly xylan. The branched groups are shed to arabinose, acetic acid, glucuronic acid, etc.

1.4.3 Lignin

Lignin is an amorphous, three-dimensional, phenylpropanoid polymer composed of methoxyphenylpropane units cross-linked by carbon-carbon and carbon-oxycarbon (Li et al., 2018), a complex phenolic polymer formed from p-coumaryl, coniferyl, and sinapyl monomers, the second most abundant organic substance in the world (Marianne et al., 2012). It crosslinks cellulose, hemicellulose, preventing the depolymerization and degradation of cellulose and hemicellulose.

1.4.4 Bioactive composition

A simple defifinition of bioactive compounds in plants is: secondary plant metabolites eliciting pharmacological or toxicological effects in human and animals (Bernhoft, 2010). According to Croteau et al. bioactive compounds of plants are divided into three main categories: (a) terpenes and terpenoids (approximately 25,000 types), (b) alkaloids (approximately 12,000 types) and (c) phenolic compounds (approximately 8000 types) (Croteau et al. 2000).

1.5 Treatment method

Although BWW contains a large number of carbohydrates and antioxidant components and is more easily hydrolyzed than most other lignocellulosic biomass, the stable cellulose-lignin-hemicellulose chemical cross-linkage structure in BWW

still poses a major obstacle to the use of BWW. Therefore, it is of great importance to strengthen the research on the treatment of BWW feedstock and to structurally modify BWW through treatment for improving the comprehensive economic benefits of BWW and the ecological environment and promote the development of low-carbon circular agriculture.

Currently, the commonly treatment methods for lignocellulose biomass can be divided for 4 categories: physical treatment, chemical treatment, physico-chemical treatment and biological treatment (Ren et al., 2016).

1.5.1 Physical treatment

The aim of physical pretreatment is mainly to reduce the particle size or crystallinity of the biomass, destroyed the cross-linked structure of cellulose, hemicellulose and lignin. The specific surface area of the biomass is increased, the contact area of microorganisms or enzymes is increased, and the degradation of part of the cellulose from the biomass is increased. Commonly used physical pretreatment methods include: mechanical crusing, microwave treatment, ultrasonic treatment etc.

(1) Mechanical crushing

The biomass is crushed by grinding and milling to make the particle size smaller, increase the specific surface area and reduce the crystallinity of the cellulose in order to improve its conversion efficiency. The advantages of mechanical crushing treatment are that it is simple to operate and easy to implement, but it is more energy intensive and costly. Therefore, the economic viability of the mechanical crushing treatment is not high and often needs to be combined with other treatment methods to reduce treatment costs.

(2) Microwave treatment

Microwave is an electromagnetic wave with a wavelength of 1 mm to 1 m and a frequency of 300 MHz to 300 GHz. Its direction and magnitude change periodically with time, and it is an electromagnetic wave with penetrating properties. The thermal effect of microwave can break the molecular structure and hydrogen bond in lignocellulose, thus increasing the specific surface area. The advantages of microwave treatment are fast reaction speed, short processing time and easy operation, while its

disadvantage is the high investment cost of equipment.

(3) Ultrasonic treatment

Ultrasound is a mechanical wave with a frequency range of 16 KHz to 16 GHz. it has cavitation effect, thermal effect and mechanical effect (Broekman et al., 2010). In liquids, ultrasonic waves of a certain intensity will produce cavitation, and due to cavitation, a large number of bubbles will be generated in the liquid, and these bubbles will break in an instant to produce a large shear force, while the acoustic energy of ultrasonic waves can form instant high temperature and high pressure conditions to break the cell wall (Broekman et al., 2010), thus increasing its specific surface area and increasing the contact area between enzymes or microorganisms and biomass, thus promoting the production of sugar or biological gas production. However, ultrasonic pretreatment is more energy intensive, costly and has severe losses, making it economically unviable.

1.5.2 Chemical treatment

Chemical treatment includes acid treatment, alkali treatment, organic solvent treatment and ionic liquid treatment, which the more commonly used treatment methods are acid treatment and alkali treatment.

(1) Acid treatment

Common treatment reagents for acid treatment include H_2SO_4 and HCl etc. The main objective is to break the chemical bonds, dissolve the hemicellulose fraction of the lignocellulose and remove the lignin to obtain cellulose. Although acid treatment is effective for lignocellulose, it can corrode equipment and is expensive to commercialise as it cannot be recycled causing acid contamination.

(2) Alkali treatment

Common treatment reagents for alkali treatment include NaOH and $Ca(OH)_2$. Alkali treatment makes cellulose more readily available by breaking intermolecular ester bonds and dissolving the lignin, but the degradation process tends to produce inhibitors, so an additional step in the detoxification process is usually required, thus increasing the cost and complexity of the production process.

1.5.3 Physico-chemical treatment

Common physico-chemical treatment methods include steam explosion (Ana et al., 2018) and ammonia fibre explosion (Farzaneh et al., 2005). These methods are similar in principle, as they all treat the fibre raw material with high temperature or pressure, and through the process of instantaneous pressure relief, the structure of the raw material is changed and the individual components are separated (Pirzadah et al., 2014), thus increasing the contact area between enzymes or microorganisms and cellulose, and accelerating the degradation of cellulose, thus achieving the treatment effect. The advantage of steam explosion treatment is that it is more environmentally friendly and no harmful substances are added, but it does not provide complete separation of the lignin and may present more inhibitors that are detrimental to fermentation (Ballesteros et al., 2002). For ammonia explosion, although less inhibition is produced, the energy consumption is higher and there is a risk of environmental pollution and personnel safety due to ammonia leakage.

1.5.4 Biological treatment

Biological treatment is a method of lignin degradation using microorganisms that break down lignocellulosic feedstock (including white rot, grey rot and soft rot bacteria), which have a unique system of breaking down lignin, secreting oxidative enzymes and whose breakdown system is selective for lignin, thereby increasing the rate of enzymatic saccharification of cellulose and hemicellulose (Ren et al., 2016). Biological treatment is an energy-saving and environmentally friendly method. Treatment with fungi prior to physical or thermochemical treatment effectively reduces the treatment time of the fungi and also reduces the harshness of the thermochemical treatment, the toxic substances and the energy requirements. However, its shortcomings are that enzyme treatment technology is still immature, fungal treatment is slow and long, and oxidase treatment efficiency is dependent on the chemical medium (Ren et al., 2016).

1.6 Principles and characteristics of subcritical liquid

Combining the shortcomings of the above treatment methods, this study based on subcritical liquid to treat lignocellulosic biomass. Subcritical liquid refers to the water

heated above the boiling point but below the critical point to treat biomass. The presence of larger ionic species and higher temperatures in subcritical liquid water synergistically facilitate the hydrolysis of organic compounds. This process only adds water or a small amount of mild chemical reagents, does not corrode the equipment, and effectively reduces energy consumption, which is a high efficiency, low cost and environmentally friendly method. Compared to supercritical water, high-temperature liquid water requires lower temperatures for the hydrolysis of lignocellulosic biomass, has longer hydrolysis times, and is more easily controllable.

During the subcritical liquid treatment, the major components of biomass (cellulose, hemicellulose and lignin) decompose into small molecules (Brand, et al. 2014). The subcritical liquid treatment can convert wet feedstock into high energy density bio-oil, water-soluble substances, char and gas at 247-374C (Elliott et al. 2015, Toor, et al, 2011, Faeth, et al. 2013). In comparison with other thermochemical processes, subcritical liquid treatment shows many advantages including: (1) the application of wet feedstock as the raw material thus avoiding the extra energy consumption to remove water; (2) eliminating the energy consumption for water vaporization; and (3) water is served as both solvent and reactant (Zhu et al 2014, Tian et al 2014, Haverly et al. 2018).

1.7 Current status of utilization of BWW

BWW is rich in fibre content and antioxidant active substances. In recent years, more and more attention has been paid to the use of BWW. BWW has been used in a variety of ways. In terms of applications, common uses for BWW include extraction of bioactive substances, as a raw material for pyrolysis of biochar or as a substrate for fermentation. Kim et al. reported that phenolic compounds can be produced or extracted from buckwheat leaves using subcritical water at different temperatures and holding times (Kim et al., 2017). Kraujalienė et al. evaluated the recovery of phytochemicals from buckwheat flowers using supercritical liquid extraction (Kraujalienė et al., 2017). Activated carbon and biochar from buckwheat hulls were prepared by Pena et al. for the catalytic purification of syngas (Pena et al., 2020). Elsayed et al. searched the effect of the methane potential of buckwheat husks and

straw in the inoculum volatile solids, inoculum to substrate ratio, and other factors (Elsayed et al., 2019). Vaickelionis et al. use of buckwheat hulls as a raw material for lightweight concrete (Vaickelionis et al., 2016). BWW has demonstrated good properties in a variety of applications.

1.8 Problems in the treatment and utilization of BWW

Although researchers have treated BWW in a variety of ways and have tried various ways to use it, there are still many problems to be solved. First, most studies have focused on either the husks, leaves, or straw of buckwheat. In industrial applications, separation of these components from one other is tedious work. Second, BWW contains many antioxidants as well as cellulose, glucose, and xylose, while few studies explored the saccharides produced from BWW. Third, most researchers have used subcritical water treatment (SWT) to extract the antioxidant components of BWW, but SWT usually requires high temperatures to achieve good extraction results, which leads to the destruction of some bioactive components at high temperatures (Castillo-Llamosas et al., 2021). Fourth,the potential of biomass processing lies in industrial scale-up. To reach large-scale BWW utilization and to assess the pilot scale, it is necessary to verify that pilot-scale reactor conditions do not change the contents of the extracted bioactive components. Finally, although a certain amount of antioxidant can be extracted from BWW, the extraction efficiency is still low and the utilization pathways to the hydrolysate is limited.

1.9 Study purpose and significance

To overcome these problems, three treatment methods and utilization route was explored in BWW. First, a SWT was considered involving the production of saccharides from BWW (mixture of husk, straw, and leaves). Second, a SEST was used as a medium to depolymerise BWW and extract the bioactive substances from BWW, and this was validated on a pilot scale. Finally, subcritical seawater treatment (SST)was used to treat BWW and the hydrolysate was used in lettuce cultivation.

1.10 Main research contents

1.10.1 SWT of BWW for sugar extraction

In the first research, a relatively mild SWT was chosen for cellulose and

hemicellulose degradation to produce saccharides from raw BWW. Moreover, the SWT of BWW resulting in the inhibition of enzymatic hydrolysis was illustrated. The sum of saccharides yields in the liquid sample were compared. The contents of cellulose, hemicellulose, and lignin were analyzed in the residue after SWT. The surface morphology of residue is observed by SEM. The irregular pores were observed after SWT due to the removal or depolymerization of some cellulose, hemicellulose, and lignin. Finally, an overall mass conversion base on saccharides production was carried out. The result reflects a considerable yield of saccharides from BWW by hydrothermal strategy.

1.10.2 BWW depolymerization using a SEST for extraction of bioactive components: from the laboratory to pilot scale

In the second research, SEST was used to depolymerize BWW and extract bioactive components such as phenolics, flavonoids, and sugars on both the laboratory and the pilot scale. On the laboratory scale, various treatment conditions were compared. Depolymerization of the microstructure was evaluated by detecting solid components, and the extraction of bioactive compounds was studied by detecting liquid components. The mechanism of SEST depolymerization of BWW and extraction of bioactive components is discussed. Scaling up to an industrial level was tested on a pilot scale, and solid and liquid components were identified. Differences between the laboratory and pilot scales were analyzed.

1.10.3 Effect of hydrolysate from SST of BWW as liquid fertilizer on lettuce growth

In the third research, BWW was treated with subcritical seawater at different treatment temperatures, and the components (such as bioactive components, ionic contents) of the hydrolysate were examined. The collected hydrolysate was used as a liquid fertilizer for lettuce growth, and finally the growth indexes and physicochemical properties of lettuce under each condition were examined.

1.11 Technical route

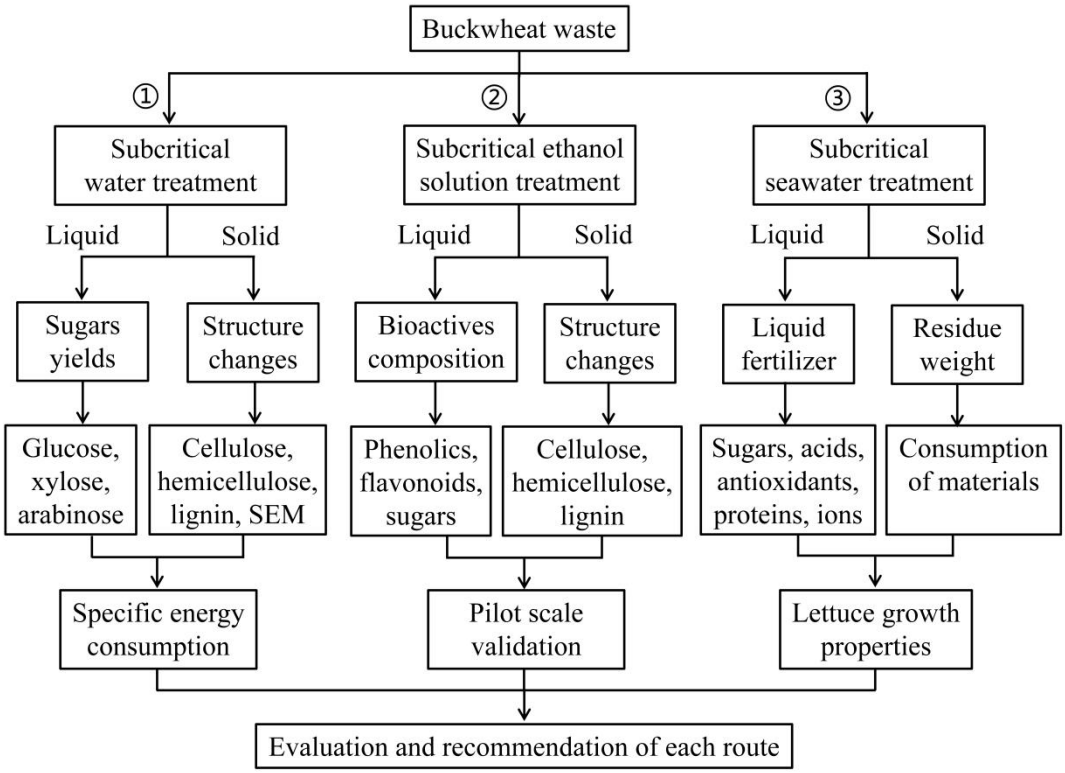

Chapter 2. SWT of BWW for saccharides production

2.1 Introduction

To realize the utilization of the valorization of BWW, a relatively mild SWT was chosen for cellulose and hemicellulose degradation to produce saccharides from raw BWW. This research used temperature and time as single factors in a full factorial experiment. The sum of saccharides yields in the liquid sample were compared. The contents of cellulose, hemicellulose, and lignin were analyzed in the residue after SWT. The surface morphology of residue is observed by SEM. Finally, an overall mass conversion base on saccharides production was carried out. The objective of this study was to provide valuable information on the utilization of BWW as a renewable resource in the biorefinery industry for the production of saccharides.

2.2 Materials and methods

2.2.1 Materials

BWW (from the Kitawase Soba variety) was obtained from the Hokkaido University test field, Sapporo, Japan, in September 2021. The dried BWW was ground in a mill, then sieved by a 40-mesh screen. The powder of BWW was dried at 25 ℃ until it reached a constant weight and was then sealed in plastic bags before storage in a drying oven at room temperature before use. A schematic diagram of the study is presented Figure 2.1.

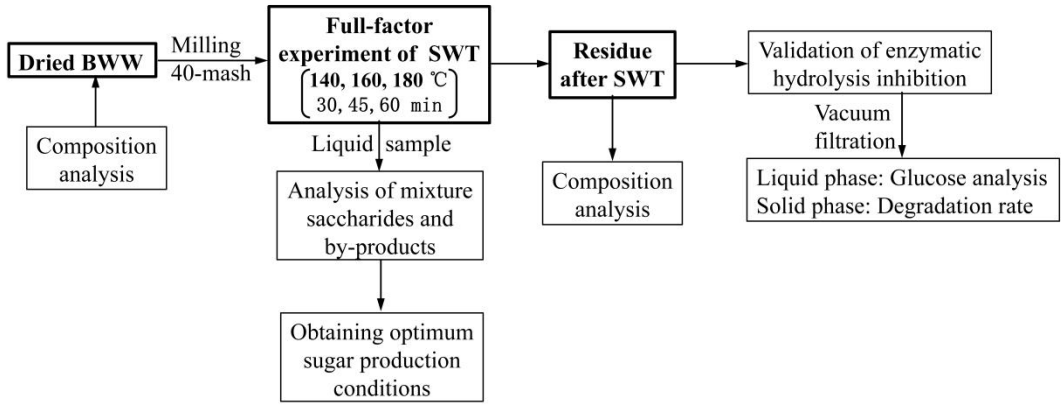

Figure 2.1 A schematic diagram for the SWT of BWW.

2.2.2 SWT extraction

SWT was performed in a 150-mL stainless-steel batch reactor (PPV-3461 Chemi-Station, EYELA, Tokyo, Japan) equipped with a heating jacket, an embedded thermometer, a magnetic agitator, and a cold-water circulation system (NCB-2500, EYELA, Tokyo, Japan). A 10.0-g sample of the raw BWW was mixed with 100 mL of distilled water and was then kept at 25 ℃ (control groups) or heated at 140, 160, and 180 ℃ and held at each temperature for 30, 45, and 60 min. The mixtures (BWW with distilled water) were heated from an initial temperature of 23 ± 1 ℃ to the target temperature at 4 ℃/min while being agitated at 500 rpm. The holding time was measured from when the target temperature was attained. The pressure within the reactor was achieved solely through the rise in temperature during the treatment. After reaction, the reactor was taken out from the heating jacket and cooled to room temperature (25 ℃) by the circulation of cold water at 5 ℃ so that the blended solid-liquid mixture could be removed. The reactor and the sample were washed by distilled water, and the solids were separated by vacuum filtration and dried in an oven at 50 ℃ to a constant weight before analysis. All experiments were repeated in triplicate.

To compare the comprehensive effects of temperature and holding time during the SWT, a severity factor (SF) defined as $\log R_0$ was introduced using the following equation (Kellock et al., 2019):

$$R_0 = t \times \exp\left[\frac{T-100}{14.75}\right] \quad (1)$$

where T is the reaction temperature (℃) and t is the holding time (min).

2.2.3 Analysis of hydrolysis products

The compositions of saccharides (glucan, xylan, cellobiose, glucose, xylose, and arabinose) and the byproducts (acetic acid, lactic acid, and 5HMF) in the hydrolysate were determined by HPLC with an RI detector (Agilent 1260 series, Agilent Technologies, Santa Clara, CA, USA) and columns for saccharides analysis: KS-802 and guard-column, KS-G 6B (Shodex). The column temperature was set at 50 ℃ with Milli-Q-grade water used as the mobile phase at a flow rate of 0.7 mL/min. For the byproducts analysis, the columns were SH-1821 and guard-column SH-G (Shodex). The column temperature was set at 60 ℃ with a 2-mmol H_2SO_4 solution as the mobile phase at a flow rate of 0.6 mL/min. The pH of the hydrolysate was determined using a WD-35634-30 digital pH meter (Oakton Instruments, Vernon Hills, IL, USA). The

3,5-dinitrosalicylic acid (DNSA) method was used to determine the reducing sugars content (Miller et al., 1959). The pH meter was validated by 4.01 (phthalate), 6.86 (phosphate), and 9.18 (tetraborate) of pH standard solution.

To consider the balance between the sum of the saccharides yield (SSY) and the energy consumption (expressed in SF), the SEC was used as an index to compare the results of the SWT experiments. The SEC was calculated as follows:

$$\mathrm{SEC} = \frac{\mathrm{SSY}\ (\%)}{\mathrm{SF}} \quad (2)$$

where SEC is the specific energy consumption of SWT for saccharides production. SSY is the sum of the yields of cellobiose, glucose, xylose, and arabinose.

2.2.4 Analysis of lignocellulose composition in residue

The lignocellulose composition of the residues, including the contents of total solids (TS), cellulose, hemicellulose, and lignin (acid-soluble lignin and acid-insoluble lignin) was determined in accordance with the (National renewable energy laboratory) NREL protocol (Sluiter et al., 2008ab). Briefly speaking, Extractives were removed by deionized water and ethanol extraction using Soxhlet method based on. Twostep acid hydrolysis was adapted for carbohydrate contents in biomass. After acid hydrolysis, hydrolyzed samples were vacuum filtered using filter crucibles. The filtrates were analyzed for carbohydrate concentration by HPLC; acid soluble lignin (ASL) was measured by spectrophotometer. The solids remained in filter crucibles were analyzed for acid insoluble lignin (AIL) and ash contents by first drying in a static oven and next ashing in a muffle oven.

The percentage solid recovery and the percentage removal of cellulose, hemicellulose, and lignin were calculated as follows:

$$\text{Solid Recovery}\ (\%) = \frac{\text{Solid after treatment (g)}}{\text{Solid before treatment (g)}} \times 100 \quad (3)$$

$$\mathrm{R_{(C,H,L)}}\ (\%) = \frac{\mathrm{m_{(C,H,L)}\ before\ treatment\ (g) - m_{(C,H,L)}\ after\ treatment\ (g)}}{\mathrm{m_{(C,H,L)}\ before\ treatment\ (g)}} \times 100 \quad (4)$$

where $\mathrm{R_{(C,\ H,\ L)}}$ is the percentage removal of cellulose, hemicellulose, and lignin, respectively, and $\mathrm{m_{(C,\ H,\ L)}}$ is the mass of cellulose, hemicellulose, and lignin, respectively.

2.2.5 Validation of the enzymatic hydrolysis inhibition of the residue after SWT

An enzymatic hydrolysis experiment on the residue after SWT and the control groups was performed to explore the inhibitory effects. A sample of residue (0.5 g) was added to 25 mL of 0.1 M sodium citrate buffer (pH = 4.8) which included 0.5 mL

of a 2 % sodium azide solution to prevent microbial contamination in a 50-mL vial. Cellulase (MP Biomedicals, LLC, Santa Ana, CA, USA) was added to the mixture at 700 U/g substrate. Before the experiment, all utensils were sterilized in an autoclave at 121 ℃ for 10 min. The mixture was heated at 50 ℃ in a shock incubator at 180 rpm for 48 h. After 6, 12, 24, 36, and 48 h, samples of the liquid were collected and centrifuged before glucose analysis by HPLC. After 48 h of hydrolysis, the residue was collected by vacuum filtration and dried at 50 ℃ until to a constant weight to calculate the rate of degradation of the substrate. For glucose analysis by HPLC, an SH-1821 column and an SH-G guard-column (Shodex, Tokyo, Japan) were used. The column temperature was set at 60 ℃ with 2 mmol H_2SO_4 solution used as the mobile phase at a flow rate of 0.6 mL/min. All of the experiments were repeated in triplicate.

The percentage degradation of the substrate after 48 h of enzymatic hydrolysis was calculated by the following equation:

$$\text{Degradation of substrate (\%)} = \frac{\text{Substrate before hydrolysis (g)} - \text{Solid phase after hydrolysis (g)}}{\text{Substrate before hydrolysis (g)}} \times 100 \quad (5)$$

2.2.6 Statistical analysis

The experimental data were presented as the means ± standard error (SE) of three replicates (n = 3). The ANOVA was performed using SPSS Statistical Software Version 25.0 to determine the statistical significance at 95 % confidence interval. All the figures were prepared using OriginPro 2021 software (OriginLab, Northampton, MA, USA).

2.3 Results and Discussion

2.3.1 Liquid fractions after SWT of BWW

In the present study, the pH decreased from 5.24 ± 0.03 to 4.23 ± 0.05 as the SF increased (Table 2.1). This could have been caused by water generating hydrogen ions under SWT due to autoionization ($H_2O \rightleftharpoons H^+ + OH^-$) (Ahmad et al., 2018) and the volatile fatty acids released or produced during SWT (Song et al., 2019), such as the acetic acid which was detected in this work. The yield of reducing sugars increased as the SF increased during SWT. The highest reducing sugars yield was 10.81 ± 0.32 % at 180 ℃ for 60 min (SF = 4.45), 2.8 times greater than the yield from the control group (25 ℃ for 60 min). Figure 2.2 shows the linear relationships between SF and the pH, reducing sugars yield and percentage solid recovery. The pH of the liquid sample and the percentage of solid recovery decreased as the SF increased. The study

Table 2.1 The chemical component, yield, and pH of the liquid sample in the first stage of different SWT conditions. Average ± s.d. significant differences occur when the alphabets are different in a column ($P < 0.05$).

Sample	SF ($LogR_0$)	pH	RS [1] (w/w%)	(Oligo- and mono-) saccharides (w/w%)				By-products (w/w%)		
				Cellobiose	Glucose	Xylose	Arabinose	Acetic acid	Lactic acid	5HMF [2]
$R_{30min\text{-}25°C}$		5.24 ± 0.03^{a}	4.03 ± 0.06^{f}	0.17 ± 0.00^{e}	1.95 ± 0.20^{a}	0.86 ± 0.04^{d}	0.10 ± 0.02^{g}	0.17 ± 0.04^{e}	0.18 ± 0.01^{e}	0.78 ± 0.002^{d}
$R_{30min\text{-}140°C}$	2.65	4.94 ± 0.05^{b}	4.82 ± 0.31^{e}	0.22 ± 0.04^{de}	1.42 ± 0.07^{c}	1.35 ± 0.39^{c}	0.14 ± 0.02^{f}	0.62 ± 0.02^{d}	0.25 ± 0.02^{de}	0.81 ± 0.002^{d}
$R_{30min\text{-}160°C}$	3.24	4.58 ± 0.04^{d}	6.25 ± 0.30^{d}	0.22 ± 0.01^{de}	1.81 ± 0.01^{b}	1.83 ± 0.07^{a}	0.25 ± 0.01^{cd}	0.83 ± 0.07^{c}	0.28 ± 0.01^{de}	0.81 ± 0.016^{d}
$R_{30min\text{-}180°C}$	3.83	4.39 ± 0.11^{e}	9.60 ± 0.80^{b}	0.45 ± 0.03^{c}	1.09 ± 0.04^{d}	1.49 ± 0.01^{abc}	0.35 ± 0.02^{a}	1.64 ± 0.30^{b}	0.56 ± 0.15^{c}	0.94 ± 0.070^{c}
$R_{45min\text{-}25°C}$		5.25 ± 0.02^{a}	4.00 ± 0.06^{f}	0.16 ± 0.02^{e}	2.01 ± 0.02^{a}	0.85 ± 0.03^{d}	0.12 ± 0.02^{fg}	0.20 ± 0.01^{e}	0.25 ± 0.03^{de}	0.78 ± 0.003^{d}
$R_{45min\text{-}140°C}$	2.83	4.83 ± 0.03^{c}	5.23 ± 0.15^{e}	0.23 ± 0.01^{de}	1.53 ± 0.02^{c}	1.56 ± 0.04^{bc}	0.14 ± 0.02^{f}	0.73 ± 0.04^{cd}	0.27 ± 0.02^{de}	0.80 ± 0.005^{d}
$R_{45min\text{-}160°C}$	3.42	4.56 ± 0.04^{d}	6.82 ± 0.21^{c}	0.26 ± 0.02^{d}	1.77 ± 0.06^{b}	1.84 ± 0.12^{a}	0.31 ± 0.01^{b}	0.83 ± 0.06^{c}	0.30 ± 0.05^{d}	0.83 ± 0.013^{d}
$R_{45min\text{-}180°C}$	4.01	4.28 ± 0.07^{f}	10.60 ± 0.30^{a}	0.70 ± 0.07^{b}	1.09 ± 0.03^{d}	1.47 ± 0.06^{c}	0.27 ± 0.00^{c}	2.16 ± 0.18^{a}	0.74 ± 0.01^{b}	1.05 ± 0.094^{b}
$R_{60min\text{-}25°C}$		5.25 ± 0.02^{a}	3.92 ± 0.20^{f}	0.16 ± 0.02^{e}	2.01 ± 0.04^{a}	0.85 ± 0.18^{d}	0.13 ± 0.02^{f}	0.20 ± 0.02^{e}	0.24 ± 0.05^{de}	0.79 ± 0.003^{d}
$R_{60min\text{-}140°C}$	2.96	4.80 ± 0.01^{c}	5.29 ± 0.19^{e}	0.22 ± 0.00^{de}	1.53 ± 0.01^{c}	1.56 ± 0.00^{bc}	0.17 ± 0.02^{e}	0.79 ± 0.01^{e}	0.29 ± 0.02^{de}	0.80 ± 0.004^{d}
$R_{60min\text{-}160°C}$	3.54	4.55 ± 0.05^{d}	6.86 ± 0.13^{c}	0.27 ± 0.02^{d}	1.69 ± 0.02^{b}	1.74 ± 0.06^{ab}	0.32 ± 0.00^{b}	0.95 ± 0.01^{e}	0.33 ± 0.07^{d}	0.84 ± 0.014^{d}
$R_{60min\text{-}180°C}$	4.13	4.23 ± 0.05^{f}	10.81 ± 0.32^{a}	0.94 ± 0.13^{a}	1.10 ± 0.05^{d}	1.43 ± 0.05^{c}	0.23 ± 0.01^{d}	2.68 ± 0.14^{e}	1.01 ± 0.08^{a}	1.12 ± 0.042^{a}

[1] RS yield, Reducing sugar yield [2] 5HMF, 5-hydroxymethylfurfural

of Batista et al. reported similar results: the SF of the sugarcane straw showed a negative correlation with mass yield and pH value after hydrothermal treatment (Batista et al., 2018). The correlation between reducing sugars yield and SF was similar to that reported for the yield of reducing sugars from corn stover after hydrothermal pretreatment (Song et al., 2019). These results showed that increasing the SF can enhance the degradation of BWW to produce reducing sugar, but will also produce some undesired byproducts (acids) at the same time.

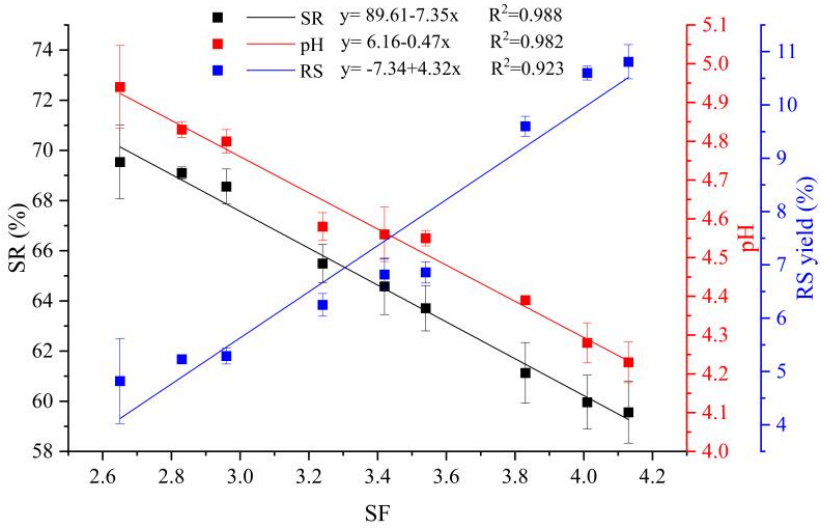

Figure 2.2 Relationships between the SF (severity factor), SR (percentage solid recovery), pH, and RS (reducing sugar) yield in the SWT of BWW under the first stage.

The components in the hydrolysate, such as disaccharides (cellobiose) and monosaccharides (glucose, xylose and arabinose), are given in Table 2.1. These saccharides were released from BWW itself and produced from the degradation of cellulose and hemicellulose by SWT (Sarker et al., 2021). Compared with the control groups, the cellobiose yield increased after SWT, gradually from 0.22 ± 0.04 % at 140 ℃ to 0.27 ± 0.02 % at 160 ℃, while there was no significant difference ($P > 0.05$). However, at 180 ℃ it clearly increased with the holding time with a significant difference ($P < 0.05$), reaching a maximum value of 0.94 ± 0.13 % at 180 ℃ for 60 min (SF = 4.13). The yields of xylose and arabinose increased as the SF increased, then decreased as the SF further increased, with maximum yields of xylose and arabinose of 1.84 ± 0.12 % and 0.35 ± 0.02 %, respectively, obtained at 160 ℃ for 45 min (SF = 3.42) and 180 ℃ for 30 min (SF = 3.83). These results appeared because a large amount of cellulose and hemicellulose could be degraded into cellobiose and monosaccharides with the increase of SF of SWT (Sarker et al., 2021), until the SF

increased to 3.42 and 3.83. Then, some xylose and arabinose were degraded to other byproducts in higher SF, resulting in a lower yield (Sarker et al., 2021; Gao et al., 2016). In contrast to the other monosaccharides, the glucose yield in the control groups was higher than that after SWT with significant difference ($P < 0.05$). Glucose comes from glucose contained in BWW itself being extracted in SWT, and from the degradation of polysaccharides such as hemicellulose.The result may be because part of the glucose released from the BWW itself was degraded during the SWT, while the amount of glucose produced by the degradation of cellulose and hemicellulose in the SWT was less than the degraded during SWT (Sarker et al., 2021). In the SWT groups, the tendency was similar to those of xylose and arabinose, with maximum yields of 1.81 ± 0.01 %, obtained at 160 ℃ for 30 min (SF = 3.24).

Some byproducts in the hydrolysate (e.g. acetic acid, lactic acid, and 5HMF) were also detected, as shown in Table 2.1. During SWT the hemicelluloses were depolymerized and degraded to furfural monosaccharides such as xylose, while some of the xylose or furfural will further degraded to HMF, and organic acids (Sarker et al., 2021; Gao et al., 2016). Compared with the control groups, only a small increase in the content of these byproducts was observed in mild SWT groups (SF = 2.65 to 3.54) ($P > 0.05$), while they dramatically increase ($P < 0.05$) with a reaction temperature of 180 ℃. The maximum yields of acetic acid, lactic acid, and 5HMF were 2.68 ± 0.14 %, 1.01 ± 0.08 %, and 1.12 ± 0.04 %, respectively, all obtained under SWT conditions of 180 ℃ for 60 min (SF = 4.13). These indicated that the conditions before 160 ℃ led to a little degradation of saccharides, yet degradation of saccharides responded extremely at 180 ℃.

The SSY (cellobiose, glucose, xylose, and arabinose) and SEC are shown in Figure 2.3. The higher SSY was obtained at 160 ℃ with a significant difference ($P < 0.05$) compared with other temperatures, while different residence time was not affected ($P > 0.05$). A maximum value of 4.18 % was achieved at 160 ℃ for 45 min (SF = 3.42). Figure 2.4 is HPLC chart for glucan and xylan as well as liquid sample. It can been seen that some peak in the liquid sample nearby the the peak of glucan and xylan. It was less than expected result because some of the polysaccharides in the hydrolyzate were not completely degraded to monosaccharides. The SEC was low at an SF of 3.83, 4.01, and 4.13, due to the degradation of saccharides to byproducts at the higher SF. Moreover, the SEC was much higher ($P < 0.05$) in the SF of 2.65, 3.24, and 3.42. The maximum SEC (1.27) was obtained at 160 ℃ for 30 min (SF = 3.24).

In this case, a relatively larger saccharides yield (4.10 %) was obtained with less energy consumption, while the byproducts yield (1.92 %) was lower with a profitable percentage solid recovery (65.49 % in Table 2.2), which could be reused in the second stage.

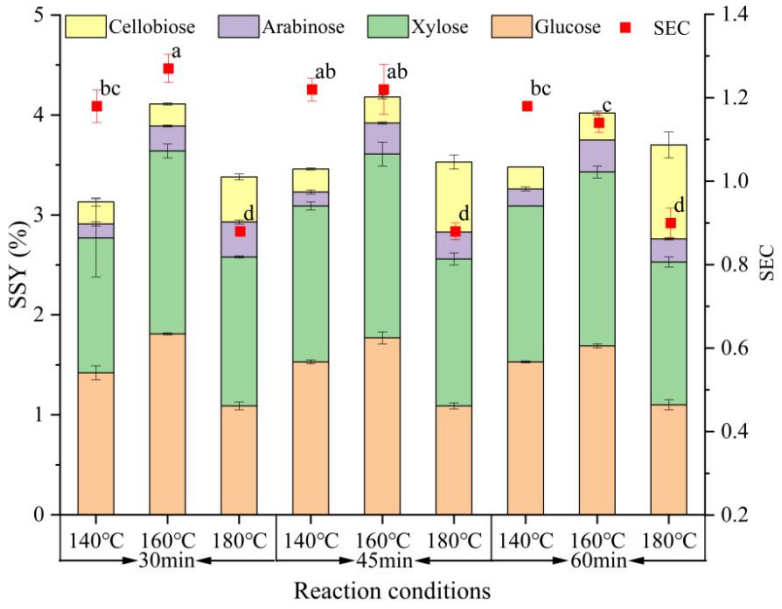

Figure 2.3 The sum of saccharides yield (SSY) in the first stage based on detected component in the liquid sample and the SEC (specific energy consumption). Significant differences occur when the alphabets are different on the bar (P < 0.05).

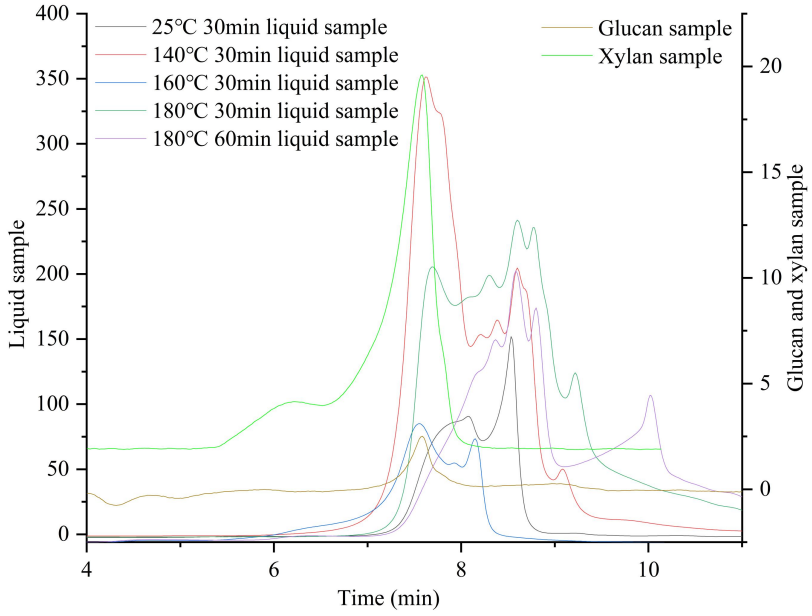

Figure 2.4 HPLC chart for glucan and xylan and liquid sample analysis.

2.3.2 The chemical composition of raw BWW and residue after SWT

The results of the composition of BWW before and after SWT under different conditions are shown in Table 2.2. The contents of cellulose, hemicellulose, lignin, and total solid (TS) in raw BWW were 27.77 ± 0.93 %, 6.06 ± 0.18 %, 26.12 ± 1.06 % (acid-insoluble lignin 17.25 ± 0.73 % and acid-soluble lignin 8.87 ± 0.73 %), and 92.82 ± 0.39 %, respectively. As the temperature and holding times increased from 25 ℃ to 180 ℃ and from 30 to 60 min, respectively, the percentage solid recovery decreased from 86.75 ± 0.85 % to 59.56 ± 1.23 %, indicating that the percentage solid recovery decreased as the SF increased. While the TS increased under different reaction conditions, the maximum of 96.06 ± 0.26 % was achieved at SWT conditions of 160 ℃ for 45 min (SF = 3.42).

These results of the chemical composition analysis of the treated BWW showed that the main component that degraded during SWT was hemicellulose. After SWT, the hemicellulose content decreased from 6.06 ± 0.18 % to 4.17 ± 0.32 %. Most hemicellulose and its degradation products converted to the liquid part after SWT. In contrast, for the raw BWW, the contents of lignin (acid-soluble lignin and acid-insoluble lignin) in the residue increased from 26.12 ± 1.06 % to 35.14 ± 1.46 % as the SF increased under the different reaction conditions. The cellulose content also increased to 30 % generally under the different reaction conditions, compared with 27.77 ± 0.93 % in the control groups. Previous studies have reported that SWT can remove most hemicellulose and increase relative cellulose and lignin content in lignocellulosic materials such as corn stover, bamboo culm, and sugarcane straw (Song et al., 2019; Batista et al., 2018; Xiao et al., 2014). The reasons may be as follows: first, hemicellulose is more easily decomposed at mild temperatures, followed by lignin, whereas cellulose is difficult to decompose at temperatures below 200 ℃ (Ando et al., 2000). Second, the decrease in hemicellulose content and increase in TS may have also caused the relative contents of cellulose and lignin to increase. Third, BWW contains a high content of antioxidants which can be transferred to the liquid phase by SWT, thereby increasing the relative contents of cellulose and lignin.

Table 2.2 The percentage of solids recovery and chemical compositions of the residue of SWT and raw BWW in second stage. Average ± s.d. significant differences occur when the alphabets are different in a column ($P < 0.05$).

Samples	SF [1] ($LogR_0$)	SR[2] (w/w, %)	Chemical composition (w/w, %)					
			Cellulose	Hemicellulose	AIL[3]	ASL[4]	Total Lignin	TS[5]
Raw BWW		100.00	27.77 ± 0.93^{e}	6.06 ± 0.18^{bc}	17.25 ± 0.73^{d}	8.87 ± 0.73^{ab}	26.12 ± 1.06^{e}	92.82 ± 0.39^{f}
$R_{30min\text{-}25°C}$		86.75 ± 0.85^{a}	30.11 ± 0.66^{dc}	6.37 ± 0.20^{abc}	20.17 ± 0.69^{c}	9.27 ± 0.30^{a}	29.44 ± 0.43^{d}	94.24 ± 0.60^{e}
$R_{30min\text{-}140°C}$	2.65	69.54 ± 0.65^{b}	26.77 ± 0.40^{e}	6.28 ± 0.77^{abc}	24.39 ± 0.78^{b}	9.00 ± 0.63^{ab}	33.39 ± 1.30^{bc}	94.77 ± 0.36^{de}
$R_{30min\text{-}160°C}$	3.24	65.49 ± 1.13^{c}	30.26 ± 0.52^{dc}	5.99 ± 0.47^{bc}	26.52 ± 0.51^{a}	8.41 ± 0.08^{bc}	34.93 ± 0.54^{ab}	95.97 ± 0.33^{ab}
$R_{30min\text{-}180°C}$	3.83	61.13 ± 1.4^{e}	31.55 ± 0.98^{abc}	4.49 ± 0.14^{d}	26.90 ± 0.79^{a}	6.42 ± 0.26^{d}	33.33 ± 0.89^{bc}	95.28 ± 0.18^{bcd}
$R_{45min\text{-}25°C}$		86.61 ± 0.24^{a}	29.61 ± 0.27^{d}	5.77 ± 0.47^{c}	20.07 ± 0.30^{c}	9.23 ± 0.35^{a}	29.29 ± 0.42^{d}	94.61 ± 0.28^{de}
$R_{45min\text{-}140°C}$	2.83	69.10 ± 0.70^{b}	26.86 ± 0.60^{e}	6.67 ± 0.17^{ab}	24.65 ± 1.02^{b}	8.98 ± 0.08^{ab}	33.64 ± 1.09^{abc}	94.87 ± 0.45^{cde}
$R_{45min\text{-}160°C}$	3.42	64.58 ± 0.76^{cd}	30.56 ± 1.56^{bcd}	5.98 ± 0.47^{bc}	26.54 ± 1.14^{a}	8.61 ± 0.33^{ab}	35.14 ± 1.46^{a}	96.06 ± 0.26^{a}
$R_{45min\text{-}180°C}$	4.01	59.96 ± 1.12^{e}	32.03 ± 1.16^{ab}	4.32 ± 0.43^{d}	27.36 ± 0.32^{a}	6.20 ± 0.37^{d}	33.56 ± 0.18^{abc}	95.55 ± 0.27^{abc}
$R_{60min\text{-}25°C}$		86.61 ± 0.90^{a}	30.46 ± 0.38^{bcd}	5.71 ± 0.61^{c}	19.89 ± 1.08^{c}	9.34 ± 0.31^{a}	29.23 ± 1.31^{d}	94.74 ± 0.59^{de}
$R_{60min\text{-}140°C}$	2.96	68.56 ± 1.21^{b}	27.98 ± 0.95^{e}	6.93 ± 0.64^{a}	24.79 ± 0.54^{b}	8.68 ± 0.26^{ab}	33.47 ± 0.29^{abc}	95.66 ± 0.50^{ab}
$R_{60min\text{-}160°C}$	3.54	63.71 ± 1.08^{d}	30.61 ± 1.88^{bcd}	6.04 ± 0.42^{bc}	27.30 ± 0.38^{a}	7.76 ± 0.71^{c}	35.05 ± 1.04^{ab}	95.91 ± 0.12^{ab}
$R_{60min\text{-}180°C}$	4.13	59.56 ± 1.23^{e}	32.80 ± 0.78^{a}	4.17 ± 0.32^{d}	26.99 ± 0.47^{a}	5.75 ± 0.26^{d}	32.75 ± 0.69^{c}	94.91 ± 0.17^{cde}

[1] SF, severity factor [2] SR, percentage solids recovery [3] AIL, acid-insoluble lignin

[4] ASL, acid-soluble lignin [5] TS, total solids content

The percentage removal of cellulose, hemicellulose, and lignin of BWW under different reaction conditions is shown in Figure 2.5. Compared with the control groups, the percentage removal of cellulose, hemicellulose, and lignin was clearly increased by SWT ($P < 0.05$), reaching maximum values of 33.17 ± 1.26 %, 59.9 ± 1.06 % and 25.33 ± 0.95 %, respectively. Cellulose still remained in the residue after SWT, which might be caused by amorphous regions of cellulose being hydrolyzed under mild SWT conditions (Himmel et al., 2008). Therefore, more serious treatment (SF > 4.13) is necessary to remove the crystalline regions of cellulose. Compared with cellulose, lignin was more susceptible to degradation under different SWT conditions. The highest percentage removal was hemicellulose under SWT conditions. However, it is possible that hemicellulose was not completely removed due to the physical obstacle of the outer edges of the cell wall, where xylan can build up and combine with cellulose (Brunecky et al., 2008).

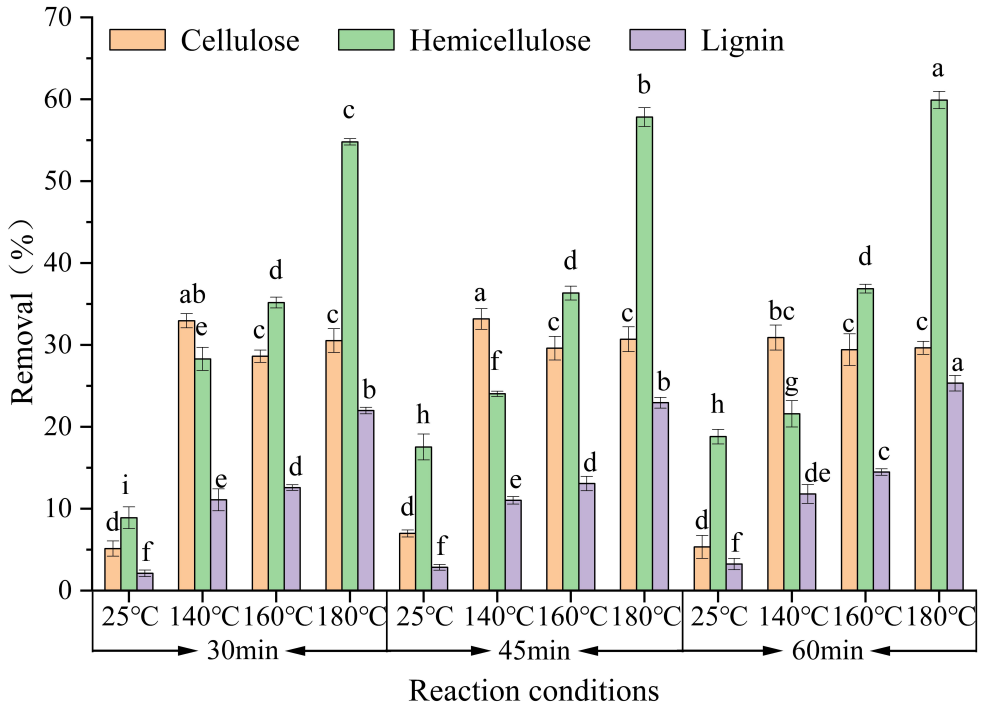

Figure 2.5 The effect of different SWT conditions on the percentage removal of lignocellulose from BWW in the second stage. Significant differences occur when the alphabets are different on the bar ($P < 0.05$).

2.3.3 Inhibitory effects of enzymatic hydrolysis of residue after SWT

Enzymatic hydrolysis of the SWT residue produced a lower glucose yield than the control groups, as shown in Figure 2.6 (A-C). The lowest glucose yield was 3.71 ± 0.59 % from residue produced at 180 ℃ for 60 min (SF = 4.13) in Figure 2.6 (C), but

it did not change greatly with different SF values. The highest glucose yield of 7.61 ±0.41 % was obtained in the control group (25 ℃ for 30 min) (Figure 2.6 (A)). These results were due to many factors affecting the enzymatic hydrolysis of lignocellulosic biomass, such as the porosity and particle size of the substrate, treatment conditions, enzymatic hydrolysis conditions, cellulose accessibility, lignin barrier, and hemicellulose content (Zhang et al., 2021). Recently, the lignin barrier has been given more research attention. The main reason for this is that nonproductive adsorption of lignin on the enzyme leads to the formation of lignin-enzyme complexes, which reduces the amount of enzymes available for cellulose degradation (Xu et al., 2020). In the present study, the high proportion of lignin in the residue after SWT may be caused by the inhibition of enzymatic hydrolysis (Table 2.2). Shen et. al. reported similar findings, in which the klason lignin yield at 180 ℃ was higher than the cellulose yield, with the saccharification lower than at 160 ℃ and 170 ℃ in enzymatic hydrolysis (Shen et al., 2016).

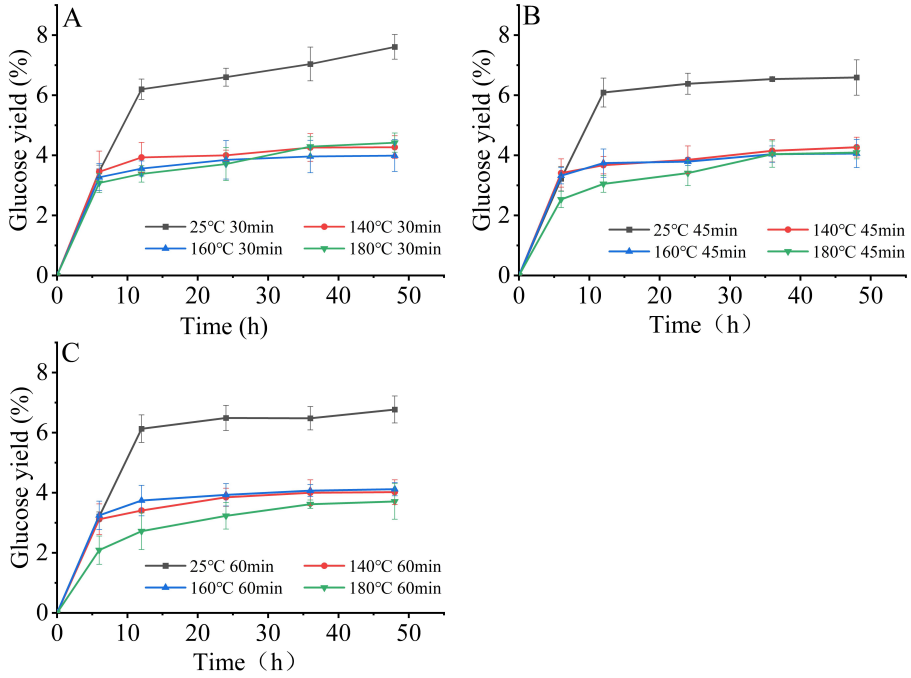

Figure 2.6 Effect of SWT conditions on the glucose yield after enzymatic hydrolysis for 48 h in the second stage. (Figure 2.6A: 30 min with different temperature of SWT, Figure 2.6B: 45 min with different temperature of SWT, Figure 2.6C: 60 min with different temperature of SWT).

Figure 2.7 shows the percentage degradation of the substrate after 48 h of enzymatic hydrolysis, illustrating that cellulose was degraded by cellulase to some

degree. The lowest degradation was 26.24 ± 1.24 % at 140 ℃ for 60 min (SF = 2.96), with no large changes for different SF values ($P > 0.05$). The highest percentage degradation was 39.19 ± 0.94 % in the control group (25 ℃ for 30 min). These data suggested that the percentage degradation in SWT residue was lower glucose production compared with those of the control group by enzymatic hydrolysis. Therefore, enzymatic hydrolysis is not advisable, as it would increase costs without achieving the desired effect of producing glucose.

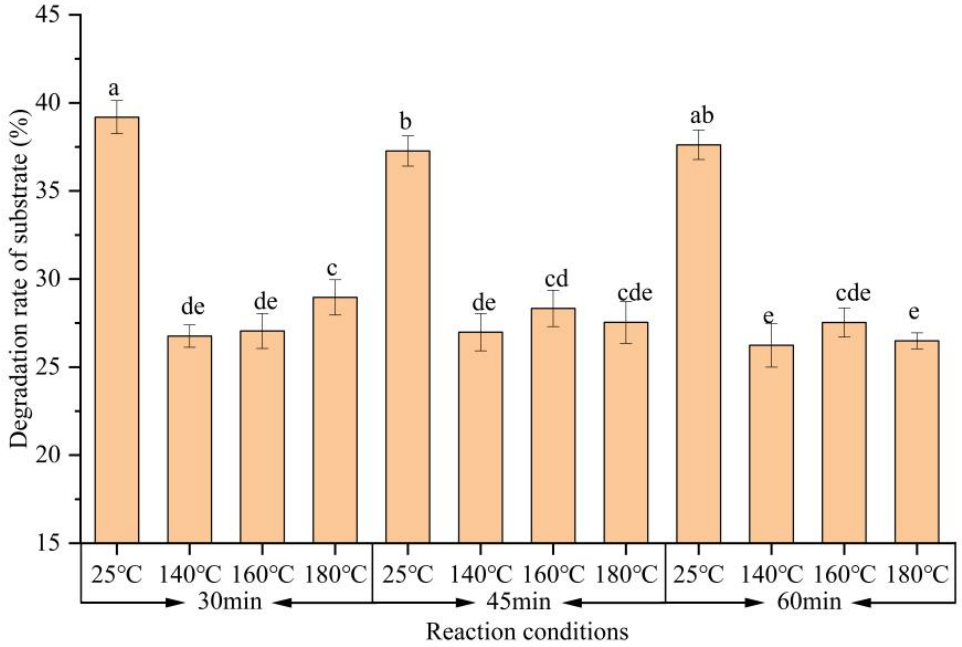

Figure 2.7 Effect of SWT conditions on the percentage degradation of the substrate after enzymatic hydrolysis for 48 h. Significant differences occur when the alphabets are different on the bar ($P < 0.05$).

2.3.4 SEM analysis

SEM images revealed the surface morphology and microstructure changes of BWW samples after SWT (Figure 2.8). The raw BWW has a flat, smooth, and compacted surface, implying cellulose was closely packed in a rigid and highly ordered manner. Cellulose is protected by a thick and smooth coating formed by the waxes and other inclusions on the surface of BWW (Shao et al., 2020). For this reason, raw BWW exhibits high recalcitrance and low accessibility of cellulase to glucan. After SWT, the BWW surface became loosen with creation of cracks and voids, due to the vast removal of hemicellulose and lignin. This result verified that SWT significantly broke the compact structure of BWW, resulted to hemicellulose and lignin removal.

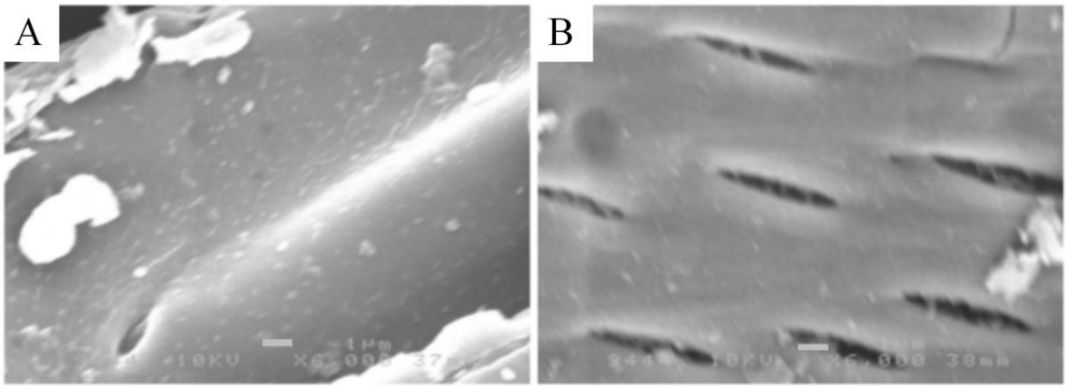

Figure 2.8 SEM images: (A) Raw BWW; (B) Residue of 160 ℃, 30 min.

2.3.5 Biomass conversion

Figure 2.9 summarizes the steps of biomass conversion during the hydrothermal process for the treatment of BWW. Initially, 10 g of milled and screened BWW consisting of 2.78 g of cellulose, 0.61 g of hemicellulose, and 2.61 g of lignin was treated by SWT at 160 ℃ for 30 min. Then the solids and liquid were separated to yield 6.55 g of residue consisting of 1.98 g of cellulose, 0.39 g of hemicellulose, and 2.29 g of lignin and liquid containing 0.41 g of mixture saccharides consisting of 0.02 g of cellobiose, 0.18 g of glucose, 0.18 g of xylose, and 0.03 g of arabinose, with 0.19 g of byproducts consisting of 0.08 g of acetic acid, 0.03 g of lactic acid, and 0.08 g of 5HMF. In this study, the SWT process from BWW is efficient for production of saccharides. Yet, unextractable carbohydrates were still present in the solid phase. Moreover, the biochar production and adsorption could still be improved. Therefore, future studies are required to improve the quantities and characteristics of the products to acquire a better technoeconomic evaluation of the whole process.

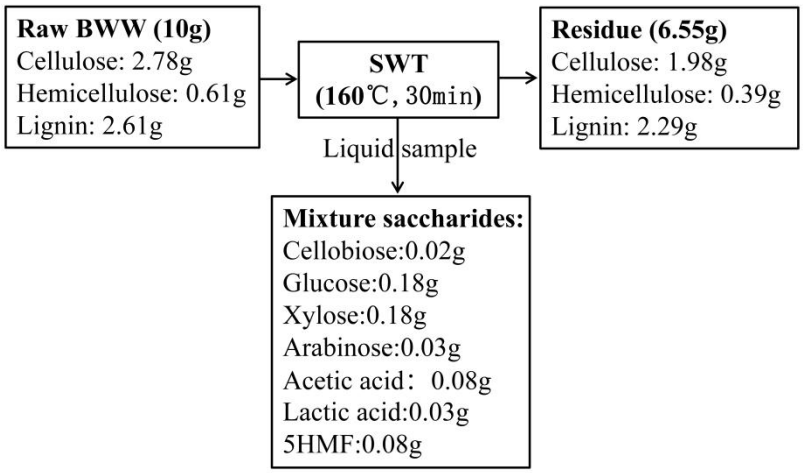

Figure 2.9 The evaluation of the biomass conversion of the SWT process.

2.4 Conclusion

In this study, saccharides production from the BWW was feasible by SWT. It revealed that the SSY was 4.10 %, with a lower total byproduct yield of 1.92 % and a relatively higher percentage solid recovery of 65.49 % under SWT conditions of 160 ℃ for 30 min (SF = 3.24). The contents of cellulose, hemicellulose, and lignin were analyzed in the residue after SWT. Enzymatic hydrolysis from the residue of SWT was inhibited. Thus, enzymatic hydrolysis for saccharides is not suitable for utilizing the residue after SWT of BWW. These results demonstrate that the SWT process is efficient for treating BWW and producing saccharides. This work lays a foundation for the industrial application of BWW, and for improving the economic benefits of buckwheat cultivation.

Chapter 3. BWW depolymerization using SEST for extraction of bioactive components: from laboratory to pilot scale

3.1 Introduction

BWW is rich in bioactive components such as antioxidants and saccharides. To effectively extract these compounds, SEST was conducted from laboratory to pilot scale. Compared with either an ethanol solution or water of subcritical treatment, SEST has lower polarity, and a higher ionic product at high temperatures (Mohamad et al., 2020). These characteristics mean that SEST can promote the depolymerization process and improve the solubility of low polarity and non-polar molecules. The use of subcritical ethanol also makes a reaction milder and less corrosive (Zhao et al., 2022). Additionally, ethanol with water under subcritical conditions can display synergistic effects that prevent condensation and gasification, which improves the conversion efficiency. Although ethanol poses an explosion risk, the ethanol used in an experiment is commonly mixed with water and the reactors are not heated with flames. Thus, adherence to proper experimental procedures reduces the risk of explosions associated with the use of ethanol to a manageable level.

Mufari et al. used a water–ethanol mixture to extract bioactive components from malted quinoa flour and observed that the temperature greatly affected extraction of active antioxidants. The maximum antioxidant activity was obtained at 200 ℃ (Mufari et al., 2021). Wu et al. treated bamboo with ethanol and water at 260 ℃ to generate bio-oil and concluded that the heating value of heavy oil decreased with increasing ethanol concentration, and the heating value of the light oil increased because of the ester exchange reaction (Wu et al., 2019). Mohamad et al. used subcritical ethanol to extract furfural from oil palm leaves (Mohamad et al., 2020). The characteristics of subcritical ethanol and the effects of ionic products and polarities on the extraction were reported for an optimum extraction temperature of 230 ℃. However, there are still problems to solve with this technique. First, structural components in cereals may differ from those of lignocellulosic biomass, resulting in applications that are not suitable for BWW. Second, differences in the high temperature conditions required for extraction may lead to different reaction pathways and intermediates. Third, the effect of extracting bioactive components under relatively mild subcritical conditions is not well understood, and the reaction mechanisms of depolymerization and extraction for specific lignocellulosic biomasses

are not known in detail. Otherwise, most research has been conducted on a laboratory scale with a low biomass. However, the potential of biomass processing lies in industrial scale-up. To reach large-scale BWW utilization and to assess the pilot scale, it is necessary to verify that pilot-scale reactor conditions do not change the contents of the extracted bioactive components.

Here, SEST was used to depolymerize BWW and extract bioactive components such as phenolics, flavonoids, and sugars on both the laboratory and the pilot scale. At the laboratory scale, various treatment conditions were compared. Depolymerization of the microstructure was evaluated by detecting solid components, and the extraction of bioactive compounds was studied by detecting liquid components. The mechanism of SEST depolymerization of BWW and extraction of bioactive components is discussed. Scaling up to an industrial level was tested on a pilot scale, and solid and liquid components were identified. Differences between the laboratory and pilot scales were analyzed. This research provides valuable information regarding the depolymerization of BWW and the subsequent extraction of bioactive components on a pilot scale.

3.2 Materials and methods

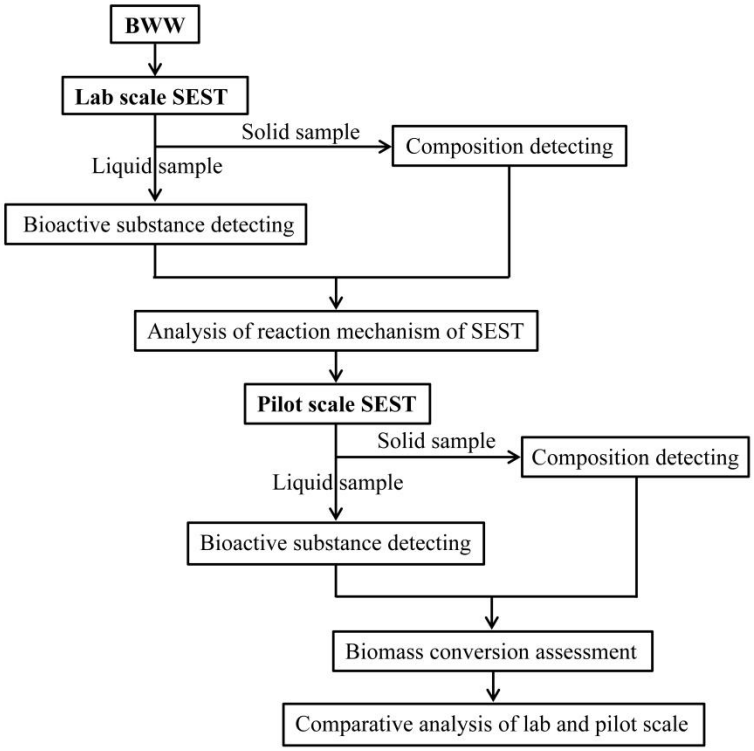

Figure 3.1 A schematic diagram of the experimental process.

3.2.1 Materials

BWW (Kitawase Soba variety) was harvested from Hokkaido University's experimental farm in Sapporo, Japan. It was rinsed with tap water, dried in air at room temperature for 20 days, cut into 5-cm pieces using a guillotine, and then dried in a drying oven at 30 ℃ until it reached a constant mass. The dried BWW was then stored in a desiccator. A schematic of the experimental process is shown in Figure 3.1.

3.2.2 Extraction experiments

3.2.2.1 Laboratory scale extraction

The prototype (Figure 3.2A) was an extraction vessel (200 mL capacity, PPV-3461 Chemi-Station, EYELA, Tokyo, Japan) equipped with an automatic control center, a heating jacket, and a cold-water circulation system (NCB-2500, EYELA, Tokyo, Japan). The maximum specifications of the system were 180 ℃ and 3 MPa. The automatic control center was used to execute the operation and control the process.

Raw BWW (5.0 g) was mixed with 100 mL of distilled water or a 50 % ethanol solution. The following five treatment groups were set up: 25 ℃ ethanol solution as control group (CK); 80 ℃ hot water (HW); 120 ℃ subcritical water (SW); 80 ℃ hot ethanol solution (E-HW); and 120 ℃ subcritical ethanol solution (E-SW). The heating period for the HW and E-HW extractions was 13 min, and that for the SW and E-SW extractions was 21 min. The operating pressure changed with increases in the temperature and maintenance period. The target temperature was maintained for 45 min. After each reaction, the reactor was cooled using circulation of cold water (5 ℃). The cooling period for the HW and E-HW extractions was 10 min, while that for the SW and E-SW extractions was 15 min. When the temperature dropped to 40 ℃, the internal pressure was released. The mixtures were then subjected to vacuum filtration to obtain the liquid fraction. The solid fraction was dried in an oven at 40 ℃ to a constant mass. All experiments were repeated in triplicate and the mean values were used.

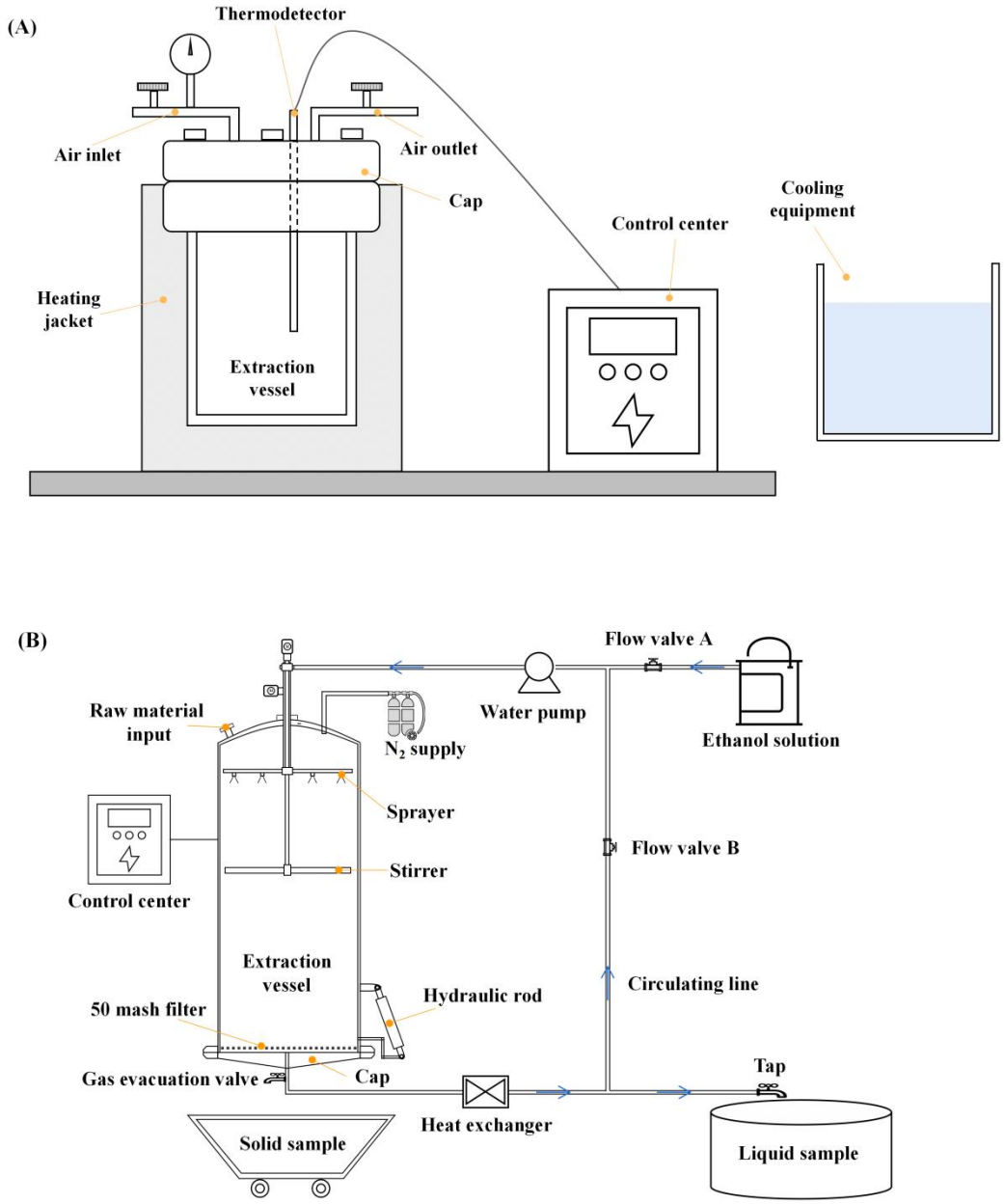

Figure 3.2 Schematic diagram of experimental equipments at laboratory scale (A) and pilot scale (B).

3.2.2.2 Pilot scale extraction

The prototype (Figure 3.2B) contained an extraction vessel (200 L capacity), an automatic control center, a heat exchanger, a liquid feeding tank, and a solid and liquid sample collector (TEX-0513, Tokyo, Japan). A heat exchanger was used to control the temperature. A water pump was used to recirculate the solution inside the reactor. A filter (50 mesh) was installed in the bottom of the reactor for solid and liquid separation. The maximum specifications of the system were 120 ℃ and 0.5

MPa. An automatic control center was used to execute the operation and control the process.

Raw BWW (5 kg) and 100 L of 50 % ethanol solution were mixed and extracted using 80 ℃ E-HW and 120 ℃ E-SW. The heating periods for the E-HW and E-SW extractions were 6 and 17 min, respectively. The operating pressure changed with increases in the temperature and maintenance period. The target temperature was maintained for 45 min. Before extraction, nitrogen was used to pressurize the reactor to approximately 0.1 MPa. At the end of the reactions, part of the pressure was released through an automatically controlled valve, the liquid was cooled one moment to 40 ℃ by a heat exchanger and then pressed to a collector by remaining pressure. The cooling period for the E-HW and E-SW extractions was around 4 min and 6 min. Finally, the bottom cap of the treatment vessel was opened and the solid was removed.

3.2.3 Analysis of the hydrolysis products

3.2.3.1 Determination of the total flavonoid and phenolic contents on the laboratory and pilot scales

Total flavonoids were detected using the colorimetric method described by Haruna et al. with a few modifications (Haruna et al., 2023). Briefly, a 0.2-mL liquid sample and 0.8 mL of distilled water were added to $NaNO_2$ (0.3 mL, 5 %). The mixture was vortexed for 6 min, then $AlCl_3$ (0.3 mL 10 %) was added. After 5 min, NaOH (2 mL, 1 mol/L) was added and the mixture was vortexed for 15 min. The total flavonoids were measured using the absorption at 510 nm. Rutin was used as a reference compound to establish a calibration curve. All samples were analyzed in triplicate. Total phenolics were detected following the Folin–Ciocalteu method described by Rajapaksha et al. with a few modifications (Rajapaksha et al., 2022). Briefly, a 0.2-mL liquid sample and 0.8 mL of distilled water were added to the Folin reagent (5 mL, 10 %) and the mixture was vortexed for 10 min. Na_2CO_3 (5 mL, 7.5 %) was added and the solution was incubated at 45 ℃ for 60 min in the dark. The total phenolics were measured using the absorption at 765 nm. A calibration curve was plotted using gallic acid as a reference compound. All samples were analyzed in triplicate.

3.2.3.2 Determination of phenolic and flavonoid components at laboratory and pilot scales

The quantities of phenolic components (p-coumaric acid, ferulic acid and gallic acid) and flavonoid components (rutin and quercetin) in the hydrolysate were determined using a high-performance liquid chromatograph equipped with an ultraviolet detector. A C18M E column for antioxidants analysis was used at a temperature of 35 ℃ (Agilent 1260 series, Agilent Technologies, Santa Clara, CA). The mobile phase was 100 % methanol (solvent A) and 0.5 % acetic acid in water (solvent B). A gradient elution was used of 30–90 % solvent A and 70–10 % solvent B over 25 min. The mobile phase flow rate was 0.8 mL/min. The injection volume was 10 μL and the components were detected at 290 nm.

3.2.3.3 Radical scavenging on the laboratory and pilot scales

The 2,2-azino-bis-3-ethyl-benzothiazoline-6-sulfonic acid (ABTS) radical scavenging abilities of the antioxidants were determined following the method of Yuan et al. (Yuan et al., 2018). The ABTS cation chromophore was prepared using a 7.4 mM ABTS solution (50 mL) and 70 mM $K_2S_2O_8$ (0.2 mL), and was kept in a dark room for 15 h. The ABTS radical solution was diluted with KH_2PO_4 buffer (75 mM, pH = 7.4) to an absorbance of 0.8 ± 0.0 at 734 nm. A 1-mL aliquot of the sample was added to 4 mL of the ABTS solution. After 6 min under incubation in a dark room, the absorbance at 734 nm was measured. The scavenging activity for ABTS radicals was calculated using the following equation:

$$\text{ABTS scavenging activity (\%)} = (1 - As/Ac) \times 100 \quad (6)$$

where As is the absorbance of the liquid sample with ABTS solution, and Ac is the absorbance of the distilled water with ABTS solution.

3.2.3.4 Reducing sugar, glucose, and xylose contents at the laboratory and pilot scales

The reducing sugars content was determined using the 3,5-dinitrosalicylic acid method (Miller et al., 1959). The glucose and xylose contents in the liquid sample were determined using a high-performance liquid chromatograph equipped with a refractive index detector. A KS-802 column with a KS-G 6B guard column (Shodex)

at a temperature of 50 ℃ was used for saccharide analysis. Milli-Q-grade water was used as the mobile phase with a flow rate of 0.7 mL/min. The sample injection volume was 50 μL.

3.2.3.5 Liquid chromatography-mass spectrometry analysis on the laboratory scale

Liquid chromatography-mass spectrometry analysis of extracts was conduct using a liquid chromatograph (Nexera-XR, Shimadzu, Kyoto, Japan) coupled with a mass spectrometer (LTQ-Orbitrap XL, Thermo Fisher Scientific, Waltham, MA). A Q-C18 column (GL Sciences, Tokyo, Japan) was used at the temperature of 35 ℃. The mobile phase was aqueous 0.1 % formic acid (solvent A) and 0.1 % formic acid in 100 % acetonitrile (solvent B) at a flow rate of 0.15 mL/min. A gradient elution was performed as follows: 0 min, 2 % B; 2 min, 90 % B; 20 min, 90 % B; 21 min, 2 % B; and 30 min, 2 % B. The sample injection volume was 5 μL.

Electrospray ionization was used in positive and negative modes. In positive mode, the source voltage was 4.0 kV, the nitrogen sheath gas flow rate was 30 L/min, the auxiliary gas flow rate was 10 L/min, the sweep gas flow rate was 0 L/min, the capillary voltage was 20 V, and the tube lens voltage was 80 V. In negative mode, the source voltage was 3.0 kV, the nitrogen sheath gas flow rate was 30 L/min, the auxiliary gas flow rate was 10 L/min, the sweep gas flow rate was 0 L/min, the capillary voltage was − 20 V, and the tube lens voltage was − 80 V. XCalibur software (version 2.0.7, Thermo Fisher Scientific) was used for data analysis.

3.2.3.6 Chemical compositions of the solid samples on the laboratory and pilot scales

The lignocellulose compositions of the solid samples, including cellulose, hemicellulose, acid soluble lignin (ASL), acid insoluble lignin (AIL), and extractives were determined using the national renewable energy laboratory protocol (Sluiter et al., 2008).

The removal rates of cellulose (RC), hemicellulose (RH), ASL (RASL), AIL (RAIL), and extractives (RE) were calculated as follows:

$$Rx\ (\%) = (m_x \text{ before treatment} - m_x \text{ after treatment})/m_x \text{ before treatment} \times 100 \quad (7)$$

where Rx is the removal rate for each component, m_x is the mass of the solid sample.

3.2.3.7 Detection mass, Brix, and turbidity on the pilot scale

Each mass was determined by weighing with a scale (IGX, ISHIDA, Tokyo, Japan) with an accuracy of ± 0.02 kg at 30 ℃. Degrees Brix values were measured with a digital refractometer (RX–5000α–Plus, Atago, Japan) with an accuracy of ± 0.010 % at 30 ℃. The turbidity was determined with a turbidimeter (FNX-80, NENTAN, Tokyo, Japan) with an accuracy of ± 2 % at 30 ℃.

3.2.4 Statistical analysis

The experimental data are presented as the mean ± standard error of three replicates. ANOVA was performed using SPSS Statistical Software (version 25.0) to determine the statistical significance at a 95 % confidence interval. The figures were prepared using OriginPro 2021 software (OriginLab, Northampton, MA).

3.3 Results and discussion

3.3.1 Laboratory scale

3.3.1.1 Phenolics and flavonoids analysis of the extracts

Total phenolics are derived from BWW and lignin degradation, whereas flavonoids are secondary metabolites of polymeric phenolic components (Shen et al., 2022). Figure 3.3A shows the total yields of phenolics and flavonoids under various reaction conditions. The total phenolics yields for the SW and E-SW extractions were significantly higher than those for the HW and E-HW extractions ($p < 0.05$), which could be attributed to the increased solubility of phenolic compounds in high temperature (Mohammadi et al., 2022). Furthermore, the higher temperature could have disrupted the BWW structure and caused degradation of more lignin to increase the total phenolics yield (Sun et al., 2021). The higher temperature may have also allowed for extraction of certain phenolics that were not extracted at lower temperatures (Rajapaksha et al., 2022). The total phenolics yield for the E-HW extraction (18.0 ± 0.9 mg/g) was significantly higher than that for the SW extraction (14.5 ± 0.7 mg/g). The E-SW extraction had the highest yield (20.1 ± 0.7 mg/g). This

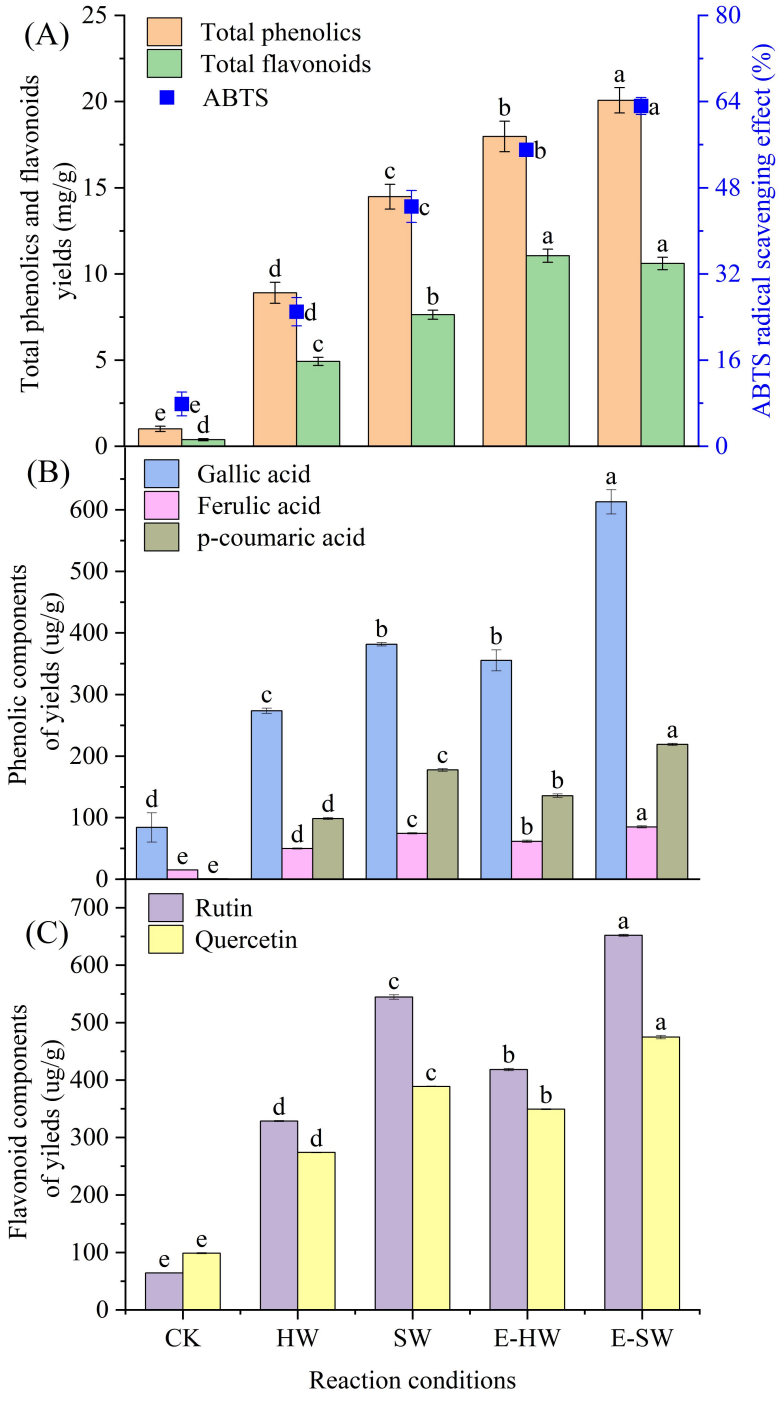

Figure 3.3 Total phenolics and flavonoids yield, as well as ABTS radical scavenging (A), phenolics yields (B), and flavonoids yields under different conditions (C). Significant differences occur when the alphabets are different on the bar ($p < 0.05$).

indicated that the total phenolics yield was more sensitive to ethanol addition than to the temperature. Ethanol would lower the dielectric constant of the solution, which would increase the solubility of the phenolics (Mohammadi et al., 2022). The total flavonoids yield for the SW extraction was higher than that for HW extraction, and the addition of ethanol increased the extraction yield, which was consistent with the results for extraction of phenolics. The total flavonoids yields for the E-HW and E-SW extractions were very similar at 11.1 ± 0.4 and 10.6 ± 0.4 mg/g, respectively ($p > 0.05$). These results indicated that there may have been some degradation of flavonoid components with the higher temperature in the presence of ethanol. The standard rutin and quercetin samples were subjected to SEST as shown in Figure 3.4. Quercetin peaks were lower for E-SW extraction than those for E-HW, and new peaks appeared at 5–7 min and at 12–15 min. Rutin peaks for E-SW were also lower than those for E-HW, and new peaks were observed at 14–16 min. This indicated that small amounts of quercetin and rutin standards sample were degraded at high temperature in the ethanol solution. The degradation results showed that there was always some flavonoid degradation in the E-SW extraction, which led to no significant difference between the total flavonoid yield for E-SW and E-HW. Lukšič et al. and Germ et al. reported that flavonoids formed complexes with proteins or straight-chain starch under subcritical conditions, which reduced their solubility in the extraction medium (Lukšič, et al., 2016; Germ et al., 2019).

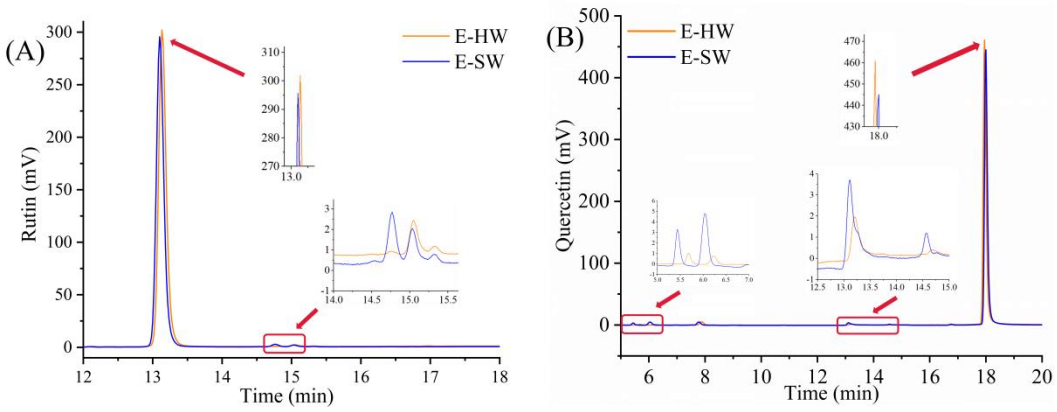

Figure 3.4 Standard curves of rutin (A) and quercetin (B) samples after E-HW and E-SW treatment.

ABTS was used to assess the antioxidant capacity (Figure 3.3A). The ABTS activity was enhanced with both the increase in the temperature and the addition of ethanol. The E-SW extraction had the highest ABTS activity (63.2 ± 1.6 %), which could be attributed to high levels of antioxidant components in the SEST. It has been reported that some sugars also have antioxidant activity (Liu et al., 2020). The reducing sugars in this study were dominated by high-molecular-weight polysaccharides, which have relatively low antioxidant activity. Figure 3.5 HPLC chart for glucan and xylan as well as the polysaccharides of liquid sample. Some polysaccharides of liquid sample nearby the glucan and xylan sample, it illustrate that have many polysaccharides are presence in liquid sample. Xu et al. reported that low-molecular-weight polysaccharides or disaccharides have stronger antioxidant properties than high-molecular-weight polysaccharides (Xu et al., 2016).

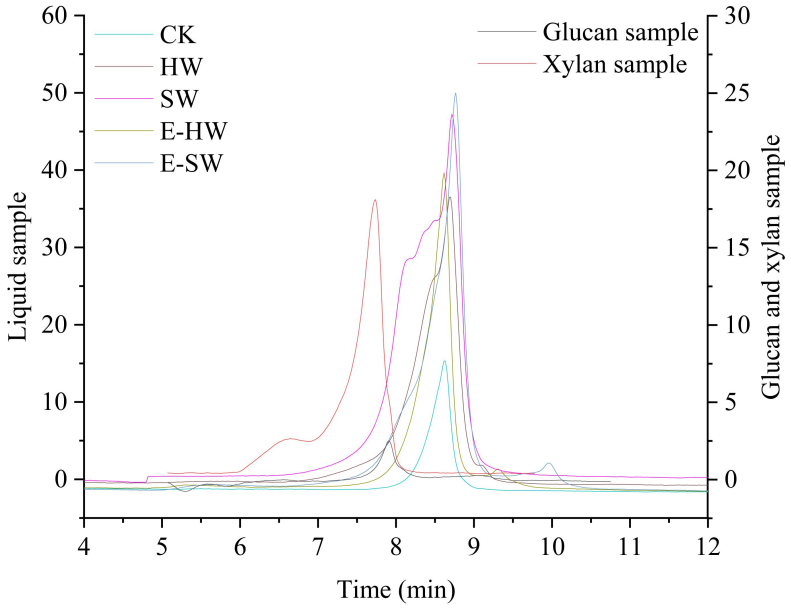

Figure 3.5 HPLC chart for glucan and xylan samples, and the polysaccharides of liquid sample.

Gallic acid, ferulic acid, and p-coumaric acid, which are common phenolic compounds were also detected (Figure 3.3B). The trends in the yields of these acids were similar, in that they all increased with the increase in temperature and the addition of ethanol. The maximum yields for gallic acid, ferulic acid, and p-coumaric acid were 612.9 ± 19.6, 85.0 ± 1.7, and 219.0 ± 1.9 μg/g, respectively, and were obtained with the E-SW extraction. The increases in the yields of these acids with the

E-SW extraction compared with the other extractions were likely caused by their increased solubility with SEST, but they could also have been caused by lignin degradation. Lignin is a polymeric phenol and its precursors are composed of p-coumaryl, coniferyl, and sinapyl monomers (Sarker et al., 2021). SEST breaks down the BWW structure and degrades lignin to produce these phenolic components.

Rutin and quercetin are common flavonoid components in BWW, and their extraction yields were also examined (Figure 3.3C). The rutin yields increased with the addition of ethanol and increase in the temperature, and the maximum yield of 652.0 ± 1.7 µg/g was obtained with the E-SW extraction. Previous studies have found that high temperatures and addition of ethanol increase the solubility of rutin and rutin-degrading enzymes, which degrade rutin into quercetin or rutinose, are inactivated under subcritical conditions (Mohammadi et al., 2022; Kalinová et al., 2018). Quercetin yield increased significantly ($p < 0.05$) with the increase in the temperature and addition of ethanol, and the maximum yield was 474.7 ± 3.1 µg/g for the E-SW extraction. Notably, the rutin and quercetin yields were relatively similar for the HW and E-HW extractions but obviously different for the SW and E-SW extractions. This could be attributed to the inactivation of rutin-degrading enzymes at high temperature resulting in no conversion of rutin to quercetin (Xu et al., 2016).

The yields of total flavonoids and phenolics were higher than the sum of the individual components (Figure 3.3). This may be attributed to the fact that bioactive components other than the ones we detected also contribute to yield. Although we did not quantify these other bioactive components, we obtained the areas of their peaks to illustrate their contribution. The peak areas of these bioactive components (Figure 3.6) showed that rutin, quercetin, gallic acid, p-coumaric acid, and ferulic acid only represented a small portion of the total bioactive components. Many other components were also present and these would contribute to the total yields of phenolics and flavonoids.

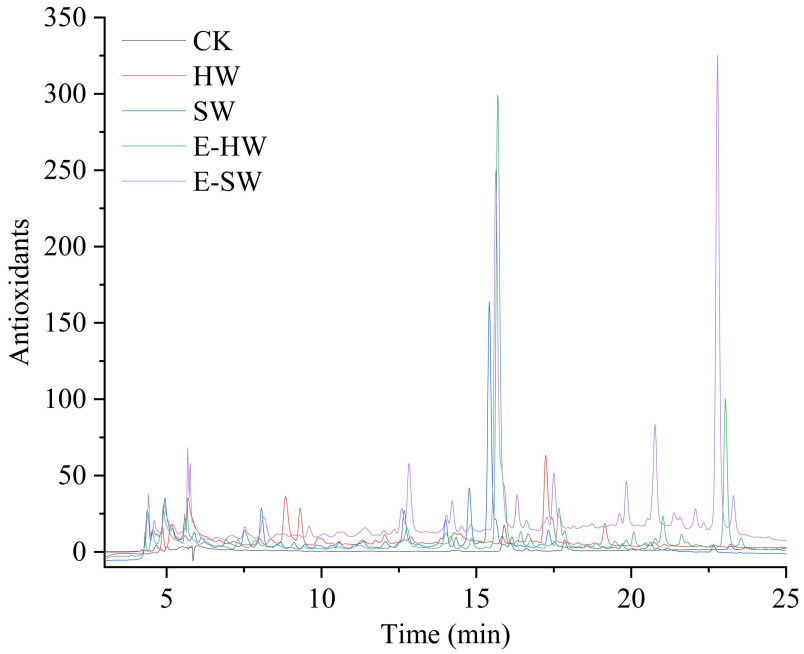

Figure 3.6 The peak of antioxidants.

3.3.1.2 Liquid chromatography–mass spectrometry analysis

Preliminary identification of several active components in the extractives of E-SW group was performed using their ionic fragments and residence times (Table 3.1 and Figure 3.7). By reviewing the literature and comparison of this results with the standard sample, the following seven phenolic components were identified: gallic acid (8), ferulic acid (4), p-coumaric acid (10), syringic acid (2), a caffeic acid derivative (3), isochlorogenic acid B (17), and a p-coumaric acid derivative (18). Seven flavonoid components were also identified. These were rutin (13), quercetin (20), catechin (9), quercetin-3-Oglucoside (12), quercetin-3-O-rutinoside (14), quercetin-3-O-hexoside (15), and quercitrin (16). Malic acid (5) and citric acid (7) were identified as other bioactive components. These results illustrate that SEST extracted a range of bioactive components that could have high value for human diet and medicinal purposes. However, SEST may also have led to the esterification of acids and alcohols to produce undesired components such as epigallocatechin 3-gallate (1) and reduce the contents of target components. This could be one reason why the total flavonoid yield for the E-SW extraction was not significantly higher than that for the E-HW extraction.

Table 3.1 Mass spectrometric data for tentatively identified compounds.

NO.	Rt (min)	Observed (m/z) $[M+H]^+/[M-H]^-$	Compounds
1	1.19	288.9	Epigallocatechin 3-gallate
2	1.4	122.9	Syringic acid
3	1.55	357.0	Caffeic acid derivative
4	1.76	387.1	Ferulic acid
5	2.17	133.0	malic acid
6	2.19	167.1	Glyceryl dimer
7	2.68	191.0	Citric acid
8	3.16	169.8	Gallic acid
9	4.22	289.2	Catechin
10	5.23	163.1	p-coumaric acid
11	5.29	161.0	D-Tagatose 2
12	5.4	303.0	Quercetin-3-o-glucoside
13	6.12	611.2	Rutin
14	6.11	609.1	Quercetin-3-O-rutinoside
15	6.36	463.1	Quercetin-3-O-hexoside
16	6.7	449.1	Quercitrin
17	7.22	191.1	Isochlorogenic acid B
18	7.62	384.1	p-coumaric acid derivative
19	7.8	631.2	Unknown
20	7.9	303.0	Quercetin
21	8.52	631.2	Unknown
22	8.51	985.3	Unknown
23	9.1	219.2	5-Hydroxytryptophan 2

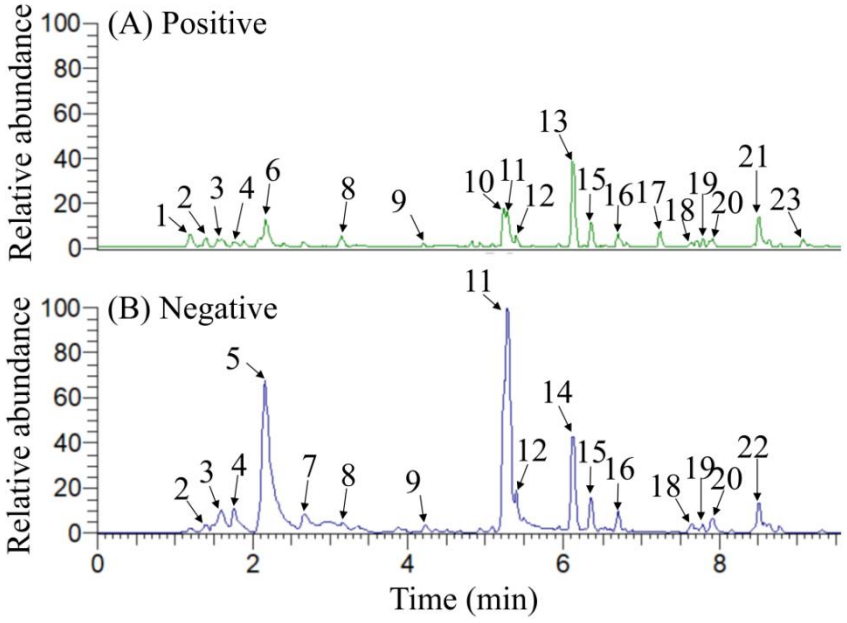

Figure 3.7 HPLC-MS spectrogram, Positive (A) negative (B).

3.3.1.3 Sugar analysis of the extract

Some of the extracted sugars in the hydrolysate originated from free sugars in the BWW and cellulose and hemicellulose degradation (Zhang et al., 2023; Alonso-Ria˜no et al., 2023; Zemnukhova et al., 2004). The reducing-sugar yields and polysaccharide peak areas for different extractions are shown in Figure 3.8A. The reducing sugars produced by BWW depolymerization were mostly polysaccharides, and most of these were high-molecular-weight polysaccharides (Figure 3.5). This may have been because the extraction temperature was low, which meant that high molecular polysaccharides could be extracted without being completely hydrolyzed into disaccharides or monosaccharides. The polysaccharide peak areas and the reducing sugar yields were significantly higher for the SW and E-SW extractions than for the HW and E-HW extractions. This could be attributed to the increase in the temperature, which would have promoted free-sugar dissolution from the BWW and degradation of starch (Alonso-Riaño et al., 2023). The reducing sugar yields for the E-HW and E-SW extractions were significantly lower than those for the HW and SW extractions. The SW extraction gave the maximum yield of 22.9 ± 0.5 mg/g. This could be attributed to the weak polarity of ethanol and the strong polarity of high-molecular-weight polysaccharides and water which means that polysaccharides are soluble in water but not in ethanol.

The amounts of xylose and glucose were also examined (Figure 3.8B). The trends for the xylose and reducing sugar yields were similar. Both yields increased only with increases in the temperature and the maximum yield of 847.7 ± 22.2 μg/g was obtained with the SW extraction. Because the amount of xylose in BWW is low, the increased yield could be attributed to the degradation of hemicellulose (Zemnukhova et al., 2004). By contrast, the glucose yield increased significantly ($p < 0.05$) with the increase in the temperature and the addition of ethanol (Figure 3.8B). The highest yield (674.3 ± 20.7 μg/g) was obtained with the E-SW extraction. This result may be attributed to the fact that water provides more H^+ during the SW, which will facilitate the conversion of glucose to furfural and lead to degradation of the dissolved glucose. However, the addition of ethanol introduced more hydroxyl groups,

which hindered the degradation of glucose and resulted in a relatively high yield for glucose. Similar results were reported by Gao et al. and Klinchongkon et al. (Gao et al., 2014; Klinchongkon et al., 2017). Gao et al. concluded that the degradation rate of glucose was faster in subcritical water than in water-ethanol mixture, and although the reason for this is not well understood, the appropriate amount of ethanol improves the stability of glucose (Gao et al., 2014). However, the amounts of glucose and xylose that was extracted from free saccharides and degraded from polysaccharides was limited, and the yield was significantly lower than that of reducing sugars. Hence, the glucose and xylose yields did not have a significant effect on the reducing sugar yield.

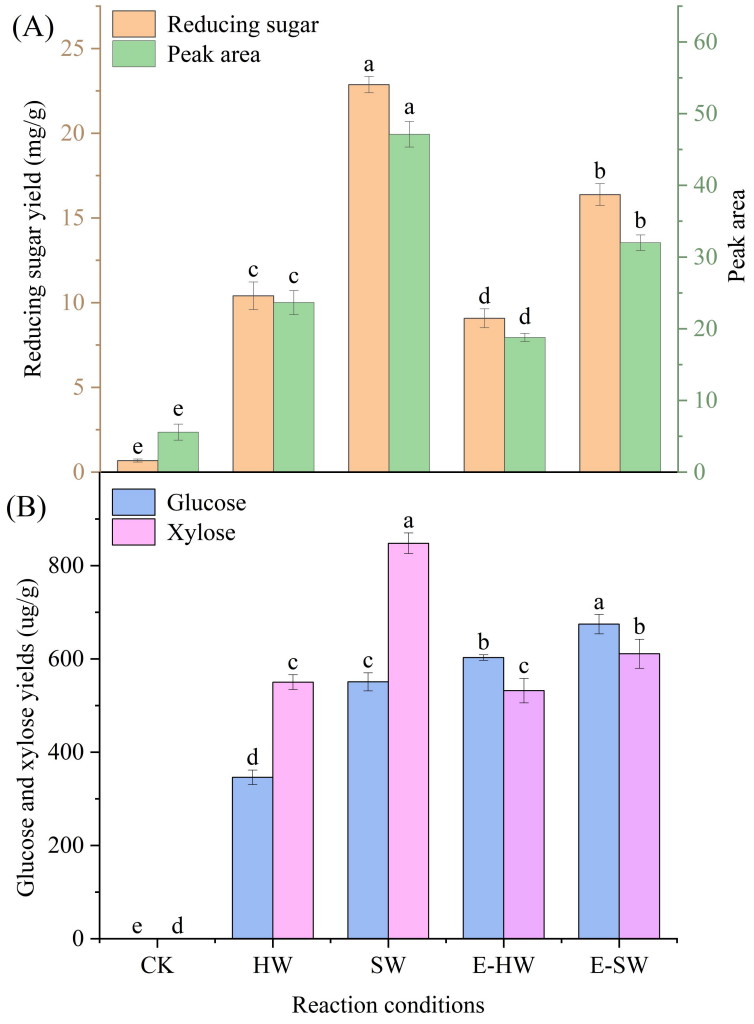

Figure 3.8 Reducing sugars yield and peak areas of polysaccharides (A), glucose and xylose yields (B) under different conditions. Significant differences occur when the alphabets are different on the bar ($p < 0.05$).

3.3.1.4. Solid sample and total hydrolysate yield analysis

Figure 3.9 shows the removal rates for cellulose, hemicellulose, ASL, AIL, and extractives. The ASL removal rate increased with the addition of ethanol, and the maximum removal rate was 13.4 ± 0.7 % for the E-HW extraction. For AIL, the removal rate was sensitive to changes in the temperature. The differences between the SW and E-SW extractions were not significant ($p > 0.05$), and the E-SW extraction gave the maximum removal rate of 8.1 ± 1.2 %. The sum of lignin removal in the E-SW extraction was significantly higher than those for the other extractions because the OH^- released by ethanol at high temperatures ruptured ester bonds between the lignin and polysaccharides, and this increased lignin depolymerization (Zhang et al., 2023). Removal of hemicellulose was significantly higher than that of cellulose and lignin because it was more soluble at mild temperature (Zheng et al., 2022). The results for the HW and E-HW extractions were not significantly different ($p > 0.05$). The result for the E-SW extraction was significantly lower than that for the SW extraction ($p < 0.05$). This indicated that ethanol exhibited limited degradation of hemicellulose, which is consistent with an earlier report (Tangkhavanich et al., 2014). Cellulose removal rates under the different conditions showed no significant differences, which was attributed to the low temperature resulting in degradation of only some of the non-crystalline cellulose and leaving most of the crystalline cellulose (Zhang et al., 2023). The cellulose and hemicellulose removal rates also verified why the yield of reducing sugars was lower for the E-SW treatment. The removal of extractives increased with increases in the temperature but did not change significantly with the addition of ethanol. This may be caused by the presence of different intermediate substances with and without ethanol. As discussed earlier in the text, SW extraction will yield more polysaccharides, and E-SW extraction will yield more phenolics. The chemical compositions of the residues are listed in Table 3.2. The contents of the extractives and hemicellulose for the E-SW extraction were relatively low compared with those for the other extractions because this treatment extracted more antioxidants and sugars and removed some hemicellulose in the SEST. The maximum cellulose content in the samples from the E-SW extraction was 37.7 ±

0.4 %. This would be beneficial for utilization of the residue, such as in enzymatic saccharification or fermentation, to meet sustainable development goals (United Nations, 2016). The total hydrolysate yields are also shown in Table 3.2. Relatively high yields were obtained under subcritical conditions because of the high temperature, while the compositions of the products were differ. Higher yields of total hydrolysate were obtained with the SW extraction compared with the other extractions, mainly because of the contribution of the reducing sugars yield. While, the maximum yield (47.1 ± 0.9 mg/g) was obtained with the E-SW extraction because this process gave higher yields of total phenolics and total flavonoids.

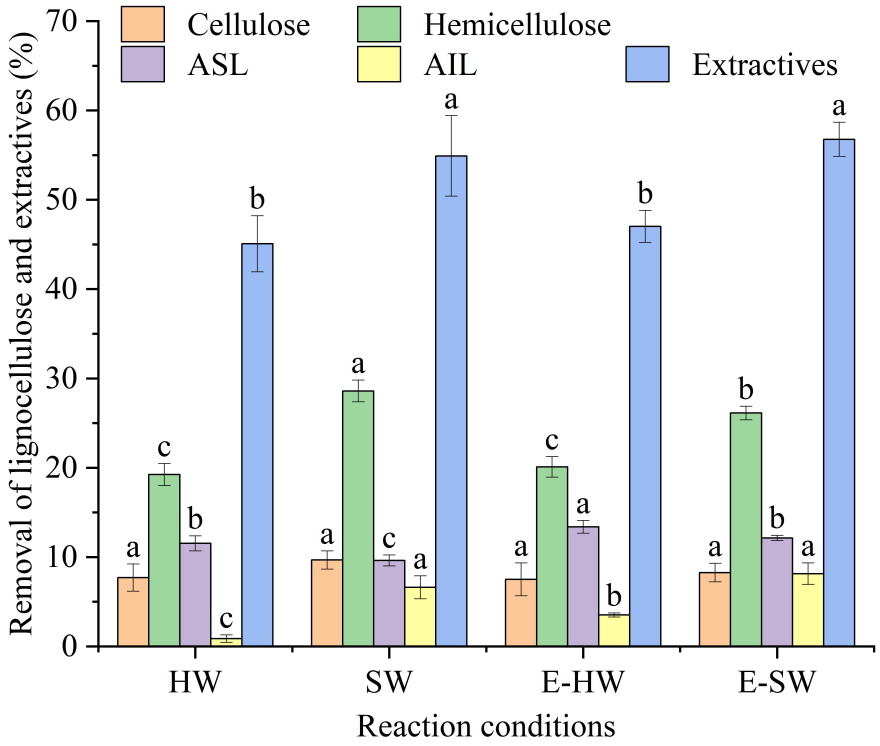

Figure 3.9 Cellulose, hemicellulose, ASL (acid soluble lignin), AIL (acid insoluble lignin) and extractives removal under different conditions. Significant differences occur when the alphabets are different on the bar ($p < 0.05$).

Table 3.2. Chemical composition of residue and total hydrolysate yield under different reaction conditions. Average ± s.d. significant differences occur when the alphabets are different in a column ($p < 0.05$).

	Extractives (w/w, %)	Cellulose (w/w, %)	Hemicellulose (w/w, %)	AIL[1] (w/w, %)	ASL[2] (w/w, %)	Total lignin (w/w, %)	Total hydrolysate yield (mg/g)
CK	12.5 ± 0.7 ^{a}	34.7 ± 0.7 ^{c}	12.3 ± 0.5 ^{a}	17.7 ± 0.2 ^{c}	9.1 ± 0.2 ^{bc}	26.8 ± 0.1 ^{d}	2.1 ± 0.3 ^{e}
HW	8.6 ± 0.7 ^{b}	36.9 ± 0.6 ^{ab}	11.5 ± 0.4 ^{b}	19.9 ± 0.4 ^{a}	9.1 ± 0.4 ^{bc}	29.0 ± 0.0 ^{ab}	24.2 ± 1.4 ^{d}
SW	7.3 ± 0.3 ^{dc}	37.5 ± 0.8 ^{ab}	10.5 ± 0.2 ^{c}	19.5 ± 0.4 ^{ab}	9.7 ± 0.0 ^{a}	29.1 ± 0.4 ^{a}	45.0 ± 0.7 ^{b}
E-HW	8.2 ± 0.6 ^{bc}	36.5 ± 0.5 ^{b}	11.2 ± 0.7 ^{bc}	19.1 ± 0.4 ^{b}	8.8 ± 0.2 ^{c}	27.9 ± 0.5 ^{c}	38.1 ± 1.0 ^{c}
E-SW	7.0 ± 0.4 ^{d}	37.7 ± 0.4 ^{a}	10.8 ± 0.1 ^{bc}	19.0 ± 0.4 ^{b}	9.3 ± 0.0 ^{ab}	28.2 ± 0.4 ^{bc}	47.1 ± 0.9 ^{a}

[1] AIL: Acid insoluble lignin [2] ASL: Acid soluble lignin

3.3.1.5 Mechanism analysis

Plant cell walls (Figure 3.10) are hierarchical structures composed of cellulose, hemicellulose, lignin (polymeric phenols), pectin, and structural proteins (Zhou et al., 2021; Hu et al., 2022). Hemicellulose is attached to cellulose via hydrogen bonds and van der Waals forces (Zhou et al., 2021; Wu et al., 2022), while lignin is attached to hemicellulose via ester bonds (Tang et al., 2017). For the phenolics, some (e.g., protocatechuic acid) are constitutes to lignin and others (e.g., ferulic acid) are attached to cellulose, lignin, or proteins via ester bonds (Meng et al., 2019). The reaction mechanism of SEST for depolymerization of BWW and extraction of the bioactive components is shown in Figure 3.10. Hydrothermal treatment can facilitate the reaction by increasing the dissociation constant and decreasing the dielectric constant (Saha et al., 2019).

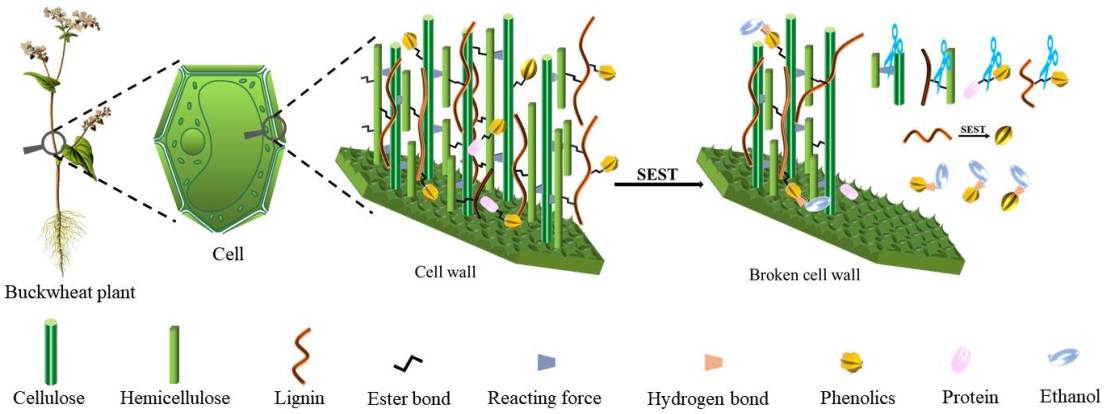

Figure 3.10 Depolymerization of BWW and extraction of bioactive components in SEST.

The dissociation constant refers to the extent to which a component dissociates into its ionic form (Zhou et al., 2018). At room temperature, water and ethanol are usually in their molecular forms, and their ionization constants are low. At 25 ℃, the ionization constant of water is 15.7 with boiling point of 100 ℃, and that ionization constant for ethanol is 16 with boiling point of 78 ℃ (Wikipedia). Only small amounts of these compounds are hydrolyzed into hydrogen ions and hydroxyl radicals. Thus, there is a shortage of the hydrogen ions and hydroxyl radicals required for the separation and degradation of cellulose, hemicellulose, and lignin. Low temperatures also do not provide sufficient kinetic energy to break the chemical bonds or forces

between and within the individual components. When the temperature increases, the ionization constant increases as more hydrogen ions and hydroxyl radicals are produced from the water and ethanol. These ions with increased kinetic energy from high temperatures break chemical and hydrogen bonds or the forces between the components of the lignocellulosic biomass for BWW depolymerization. A portion of the cellulose, hemicellulose, and lignin produced by depolymerization is further hydrolyzed to produce monomeric components (Zhou et al., 2021; Hu et al., 2022). Hydrothermal reactions also involve recombination of intermediates that are potentially detrimental, such as pseudo-lignin (Jiang et al., 2022). However, the hydroxyl groups in ethanol attack the ether bonds in the lignocellulosic structure to form phenol, which acts as a capping reagent that reacts with intermediates produced by lignin degradation to prevent repolymerization, which presents a synergy between the water and ethanol (Zhao et al., 2022,Yuan et al., 2010). Hence, removal of lignin in the E-SW extraction was significant and the phenolic yield was high. Ethanol reportedly has a good hydrogen supply capacity (Zhao et al., 2022); here, however, the hydroxyl radicals from ethanol are important because they break ester bonds between lignin and hemicellulose and increase the lignin removal while selectively retaining cellulose and hemicellulose (Zhang et al., 2023). Gu et al. also reported that ethanol hindered sugar degradation but increased lignin solubilization (Gu et al., 2022).

The dielectric constant refers to the ability of a material to retain its charge, and is important in separation techniques (Deng et al., 2022). At 20 ℃, the dielectric constant of water is 80.0, and that for ethanol is 25.0 (Mohsen-Nia et al., 2010). When ethanol was added to water, the dielectric constant of the solution was lower than that of pure water. Thus, the solution had a lower electron retention ability and a lower polarity than pure water. Therefore, hydrogen bonds formed more readily between bioactive components that were non-polar or had low polarity and the water–ethanol solution, which resulted in extraction of these antioxidants. However, relative to SEST, the dielectric constant of the room-temperature ethanol solution was high and the hydrogen bonds were weak. Thus, a subcritical ethanol solution was used. With an

increase in the temperature, the dielectric constant of the ethanol solution and the ability to retain electrons both decreased. The low polarity greatly increased hydrogen bonding between ethanol and phenolics (Figure 3.10). Therefore, SEST increased the yields of these bioactive components relative to the room-temperature ethanol solution and hydrothermal treatment.

3.3.2 Pilot-scale analysis

3.3.2.1 Extraction of bioactive components and removal of solids

Table 3.3 lists the yields of bioactive components for the pilot-scale E-HW and E-SW extractions. The trends were similar to those observed in the laboratory-scale experiments. The E-SW extraction gave significantly ($p < 0.05$) higher yields of total phenolics and reducing sugars than the E-HW extraction. The maximum total phenolics yield was 29.8 ± 0.1 g/kg, and that of reducing sugars was 33.9 ± 0.5 g/kg. The total flavonoids yield for the E-HW extraction was higher than that for the E-SW extraction. The lignocellulose removal with the E-SW extraction was significantly ($p < 0.05$) higher than that with the E-HW extraction (Table 3.4).

Table 3.3 Bioactive components yield of E-HW and E-SW in pilot scale.

	E-HW	E-SW	Statistical significance
Total phenolics (g/kg)	23.2 ± 0.4	29.8 ± 0.1	$p < 0.001$
Total flavonoids (g/kg)	14.9 ± 0.2	13.9 ± 0.5	$p = 0.031$
Reducing sugar (g/kg)	25.0 ± 0.7	33.9 ± 0.5	$p < 0.001$
Gallic acid (mg/kg)	664.9 ± 6.8	777.9 ± 17.1	$p < 0.001$
Ferulic acid (mg/kg)	84.9 ± 0.2	111.0 ± 0.1	$p < 0.001$
p-coumaric acid (mg/kg)	200.9 ± 1.8	259.7 ± 1.0	$p < 0.001$
Quercetin (mg/kg)	460.6 ± 1.9	554.1 ± 3.8	$p < 0.001$
Rutin (mg/kg)	658.1 ± 2.3	769.3 ± 1.7	$p < 0.001$
Glucose (mg/kg)	1973.8 ± 19.5	2035.0 ± 30.9	$p = 0.044$

Table 3.4 Lignocellulose removal of E-HW and E-SW in pilot scale (%).

	E-HW	E-SW	Statistical significance
Cellulose	6.9 ± 0.3	8.5 ± 0.9	$p = 0.038$
Hemicellulose	23.3 ± 1.4	27.4 ± 0.7	$p = 0.012$
Lignin	9.0 ± 0.6	10.6 ± 0.5	$p = 0.029$
Extractives	52.2 ± 0.6	55.9 ± 0.2	$P < 0.001$

3.3.2.2 Turbidity, Brix, and mass analysis of the liquid samples

The turbidity values, Brix values, and masses of the hydrolysates are listed in Table 3.5. The formazin turbidity unit represents the solution turbidity. In this study, the formazin turbidity unit was higher with the E-SW extraction than in the E-HW extraction. These results indicated that the E-SW extraction broke down the BWW cross-linked structure into smaller particles or produced a suspension of cellulose, hemicellulose, and lignin in the hydrolysate (Figure 3.10). The Brix value represents the percentage of soluble solids in a solution. The samples from the E-HW extraction had lower Brix values than those from the E-SW extraction. The soluble components usually include polysaccharides, polymeric phenols, and amino acids. Therefore, the E-SW extraction facilitated the degradation and solubilization of BWW structural. Interestingly, the E-SW extraction promoted BWW depolymerization and increased the yields of total phenolics and flavonoids. However, the liquid sample masses in the E-SW group decreased. This was attributed to the higher temperature, which increased both the penetration of ethanol into the lignocellulosic biomass and the contact area between the ethanol and the biomass. Consequently, more ethanol and water molecules formed hydrogen bonds with the lignocellulosic biomass, which meant that ethanol and water were retained in the solid (Figure 3.10).

Table 3.5 Turbidity, Brix and mass of the liquid samples.

	E-HW	E-SW
Liquid weight (kg)	91	83
Brix (%)	18.8	19.2
Turbidity (FTU)	118	445

3.3.2.3. Biomass conversion

Figure 3.11 summarizes the BWW biomass conversion in the pilot-scale SEST. Initially, 5 kg of BWW consisting of 1.80 kg of cellulose, 0.67 kg of hemicellulose, 1.40 kg of lignin, and 0.72 kg of extractives was treated in the E-SW extraction. Then, the solid and liquid fractions were separated. The liquid fraction contained 0.07 kg of total flavonoids, 0.15 kg of total phenolics, and 0.17 kg of reducing sugars. The solid fraction contained 1.68 kg of cellulose, 0.49 kg of hemicellulose, 1.25 kg of lignin, and 0.32 kg of extractives. The SEST depolymerized BWW and extracted the

bioactive components; however, some polyphenolics were present in the solid fraction because of the low extraction temperature and large size of the particles in the BWW feedstock. Hence, further studies are required to improve the feasibility of the entire process and increase the bioactive component yields to improve the economics.

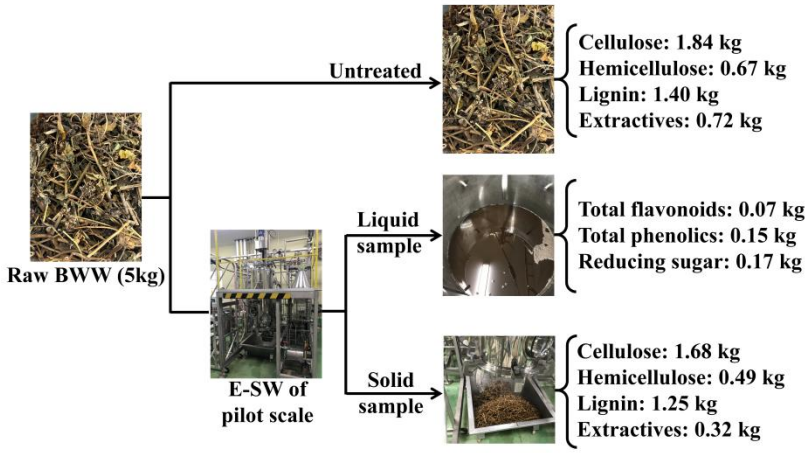

Figure 3.11 BWW biomass conversion in pilot-scale SEST.

3.3.3 Analysis of the reasons for the difference in yields in laboratory and pilot scale

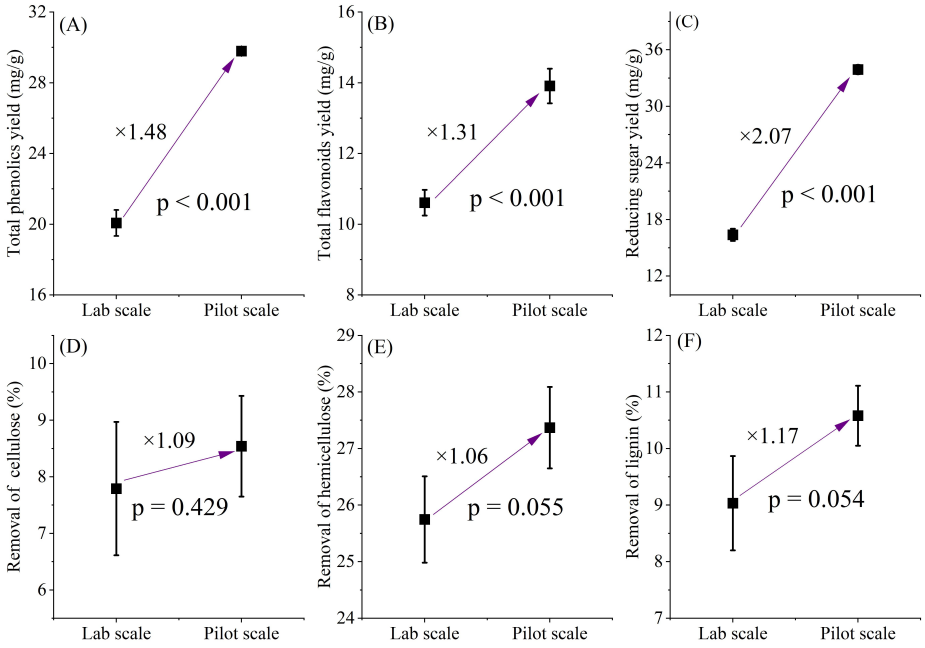

Figure 3.12 Comparison of lab- and pilot-scale experiments. The total yield of phenolics (A), flavonoids (B), and reducing sugars (C). Removal of cellulose (D), hemicellulose (E), and lignin (F).

The pilot scale performed better than the laboratory scale in terms of the yields of bioactive components and removal of lignocellulose. A comparison analysis of the SEST results for the laboratory and pilot scales is shown in Figure 3.12. This difference in performance was attributed to the following reasons:

(1) The increase in scale allowed for more complete and homogeneous reactions. The BWW (5 g) used in the laboratory scale was uniform and the particles were approximately 5 cm in size. The 5 kg of BWW used in the pilot scale contained particles that were smaller than 5 cm, which enabled more complete extraction (Essien et al., 2020).

(2) The effect of the temperature increase during the extraction was higher for the pilot scale than for the laboratory scale. The temperature inside the laboratory-scale reactor was only 80 ℃ after 5 min. By comparison, the temperature in the pilot-scale reactor reached 115 ℃, which was close to the target temperature (Figure 3.13). Thus, the extraction period of bioactive components near the target temperature was longer in the pilot-scale reactor (Essien et al., 2020). Alonso-Riaño et al. found through analysis of the results that differences in heating rates between the laboratory scale and the pilot scale affect the yield of bioactives from hydrothermal treatment of brewery spent grain (Alonso-Riaño et al., 2023).

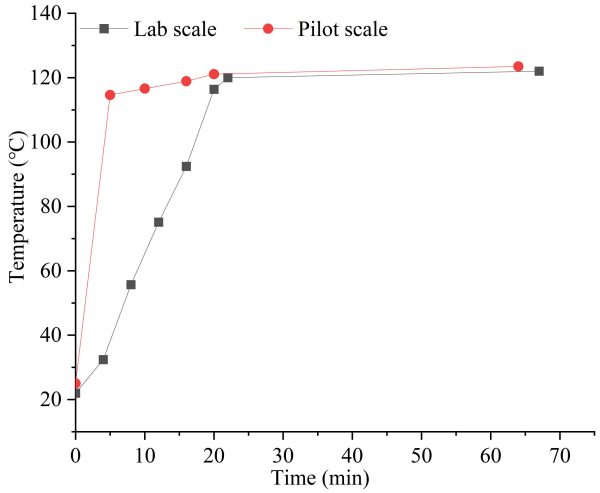

Figure 3.13 The temperature rise rate during the extraction process of laboratory and pilot scale.

(3) Under the pilot-scale conditions, 0.1 MPa of nitrogen gas was added for safe operation and pressing the liquid sample out. This could have prevented oxidation of

the antioxidants and increased their yields. The increase in pressure may have also facilitated degradation of the BWW structure by increasing the kinetic energy of the molecules and promoting extraction of the bioactive components (Essien et al., 2020).

(4) The pilot-scale reactor contained an internal sprayer for circulating water (Figure 3.2B). The slow flow of the ethanol solution increased the kinetic energy of the bioactive components. This energy led to increased and faster flow of the bioactive components into the liquid, which facilitated the extraction.

(5) There was a difference in the ratio of used-to-free space. In the laboratory-scale experiment, the ratio of used-to-free space was 2:1, whereas that in the pilot-scale experiment was 1:1. This may have led to different pressures for bioactive component extractions on the different scales; however, further study is required to confirm this. These analyses suggest that new influencing factors can emerge when scaling up. In scale up experiments, attention is needed not only for factors such as temperature and time, but also for feedstock homogeneity, ways of heating the equipment, and even the flow of the internal liquid.

3.4 Conclusions

SEST could depolymerize BWW and extract bioactive components better than hydrothermal treatment or low temperature treatment with an ethanol solution. The total phenolics content increased significantly because SEST promoted the degradation of lignin and the solubilization of extractives. The yield of total flavonoids did not change significantly with increases in the temperature, which could be attributed to degradation of some flavonoid components at high temperature. Reducing sugars were mainly in the form of polysaccharides, which was attributed to the low temperature. The yield of reducing sugars in the SEST group was lower than that in the SWT group because cellulose and hemicellulose was retained in the SEST treatment. These results provide a reference for subsequent biorefining. Differences in equipment parameters and material homogeneity in scale-up can affect experimental results. The maximum total yields of phenolics, flavonoids, and reducing sugars were 29.8 ± 0.1, 13.9 ± 0.5 and 33.9 ± 0.5 g/kg, respectively. This preliminary study provides valuable reference data for BWW utilization on a pilot scale.

Chapter 4. Effect of hydrolysate from SST of BWW as liquid fertilizer on lettuce growth

4.1 Introduction

Approximately 97 % of the Earth's water resources consist of seawater (Yang, 2020). It is abundant, easily accessible, cost-effective, and rich in inorganic salts. The metal ions present in seawater provide indirect weak acidity, facilitating the degradation of hemicellulose into disaccharides. Chloride ions in seawater can break hydrogen bonds in polysaccharides, promoting the degradation of polysaccharides into monosaccharides (Zhang, 2020). Therefore, in recent years, seawater has gained increasing attention and has been used as a catalyst to enhance the decomposition of lignocellulosic biomass (Fang, 2015). However, it has been reported that the enzymatic hydrolysis of lignocellulosic biomass after seawater hydrothermal pretreatment does not yield satisfactory results. The residual cations and anions in the solid phase after pretreatment may have some inhibitory effects on enzyme activity and behavior (Zhang, 2020). This indicates that in the process of SST of lignocellulosic biomass, the biomass acts as a biochar, adsorbing inorganic salts from seawater, thus desalinating the water and releasing organic components such as carbohydrates, antioxidants into the liquid phase. These carbohydrates, antioxidants, and appropriate amounts of metal ions are beneficial constituents in plant cultivation. These extracts can alleviate salt stress, possess antibacterial properties, and promote plant growth (Aydin et al. 2012, Tran et al. 2020, Khoulati et al. 2019, Hassan et al. 2020). Aydin et al. fund that humic acid application alleviate salinity stress of bean plants (Aydin et al. 2012). Tran et al. explored that the growth promotion effect of microelement fertilizers containing low molecular weight chitosan and xanthan on radish (Tran et al. 2020). Khoulati et al., researched the saffron extract stimulates growth, improves the antifungal effect of solanum (Khoulati et al. 2019). Hassan et al. discussed the mitigation of salt-stress effects by moringa leaf extract or salicylic acid through motivating antioxidant machinery in damask rose (Hassan et al. 2020). However, to date, there have been no reports on the application of hydrolysate obtained from SST of BWW as liquid fertilizer in plant growth.

In this study, the hydrolysate from SST of BWW was utilized in lettuce cultivation. Different treatment temperatures (110 °C, 170 °C, and 230 °C) were employed for the SST of BWW, and the composition of organic compounds (such as antioxidant components, carbohydrates, proteins) and the content of metal ions (such as calcium, magnesium, potassium, sodium, etc.) in the hydrolysate were determined. The collected hydrolysate under each temperature condition was applied as liquid fertilizer in lettuce cultivation, and the growth parameters of lettuce were subsequently evaluated. This study combines the utilization of biomass and seawater for agricultural cultivation, providing a new approach for the utilization of lignocellulosic biomass and serving as a reference for seawater irrigation in agricultural practices. Additionally, it enhances the added value of buckwheat cultivation.

4.2 Materials and methods

4.2.1 Materials

BWW (from the Kitawase Soba variety) was obtained from the Hokkaido University test field, Sapporo, Japan, in September 2021. The dried BWW was ground in a mill, then sieved by a 40-mesh screen. The powder of BWW was dried at 25 ℃ until it reached a constant weight and was then sealed in plastic bags before storage in a drying oven at room temperature before use. A schematic diagram of the study is presented Figure 4.1.

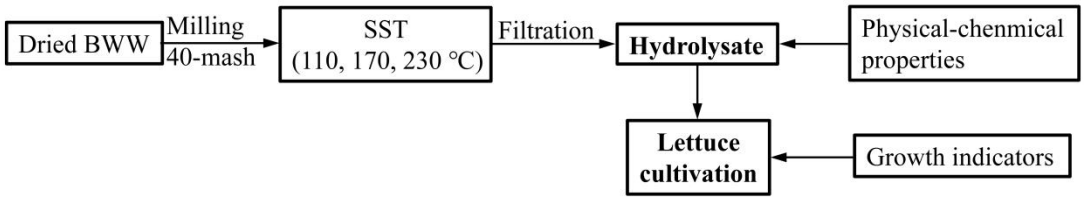

Figure 4.1 The schematic diagram of this study.

4.2.2 SST experiment

BWW was sourced from experimental fields at Hokkaido University, and seawater was obtained from the Zenibako coast, Japan (longitude 141°12'14" E, latitude 43°9'24" N). The experiments were conducted in a 200 mL reaction vessel

(PPV-3461 Chemi-Station, EYELA, Tokyo, Japan). A mixture of 6 g BWW and 150 mL seawater was reacted at temperatures of 110 °C, 170 °C, and 230 °C for 45 minutes (We denote these three groups of experiments as $H_{110°C}$, $H_{170°C}$, $H_{230°C}$), with a stirring speed of 800 rpm. CK as the control group, only use seawater as the fertilizer. After completion, the reaction vessel was cooled to room temperature by placing it in cold water. Subsequently, the resulting solid-liquid mixture was centrifuged at 8000 rpm for 20 minutes to separate the solid and liquid phases. The volume of the liquid phase was measured using a graduated cylinder and stored at 4 °C until further use, while the residual solid was collected and dried at 50 °C until constant weight. Each experiment was repeated 10 times under each temperature condition, and the resulting hydrolysate from the 10 repetitions was combined for subsequent usage and analysis.

4.2.3 Lettuce cultivate experiment

Lettuce 'Grand Rapids' seeds were purchased from the Sakata Seed Corporation Ltd. (Yokohama, Japan). The experiment was conducted under natural conditions in a plastic-film greenhouse on the campus of Hokkaido University (43°4′ N, 141°20′ E; 20 m above sea level). The seeds were washed and soaked in warm water at 55 °C for 5 min and then wrapped in wet gauze to accelerate germination for 48 h at 25 °C. After germination, the seeds were sown in a seeding tray with 40 cells (7cm×7cm) and one seeds per cell on 12 April. Commercial nutrition soils were used as seedling medium and purchased from the Iris Ohyama Corporation Ltd. (Sendai, Japan). Uniform healthy seedlings were selected at 20 days and starting from now, fertilization will be conducted using hydrolysates under different temperature conditions, while the control group will utilize seawater. A pot experiment was performed using a completely randomized factorial design. Each experimental group consisted of 7 lettuce plants. The fertilizer was diluted to a concentration of 8.33 % by mixing 10 mL of liquid fertilizer with 1190 mL of distilled water. A daily irrigation of 40 mL of the diluted fertilizer was applied. The plants were continuously irrigated for 18 days, after which the growth parameters of the plants were measured and harvested.

4.2.4 Analysis of hydrolysate composition

4.2.4.1 Reducing sugars content

The reducing sugars content was determined by 3,5-dinitrosalicylic acid method (Miller et al., 1959).

4.2.4.2 Total flavonoid contents

Total flavonoids were detected using the colorimetric method described by Haruna et al. with a few modifications (Haruna et al., 2023). Briefly, a 0.2-mL liquid sample and 0.8 mL of distilled water were added to $NaNO_2$ (0.3 mL, 5 %). The mixture was vortexed for 6 min, then $AlCl_3$ (0.3 mL 10 %) was added. After 5 min, NaOH (2 mL, 1 mol/L) was added and the mixture was vortexed for 15 min. The total flavonoids were measured using the absorption at 510 nm. Rutin was used as a reference compound to establish a calibration curve. All samples were analyzed in triplicate.

4.2.4.3 Total phenolic contents

Total phenolics were detected following the Folin–Ciocalteu method described by Rajapaksha et al. with a few modifications (Rajapaksha et al., 2022). Briefly, a 0.2-mL liquid sample and 0.8 mL of distilled water were added to the Folin reagent (5 mL, 10 %) and the mixture was vortexed for 10 min. Na_2CO_3 (5 mL, 7.5 %) was added and the solution was incubated at 45 ℃ for 60 min in the dark. The total phenolics were measured using the absorption at 765 nm. A calibration curve was plotted using gallic acid as a reference compound. All samples were analyzed in triplicate.

4.2.4.4 Total acid contents

5mL of sample diluted 5 times with 15mL of water and 100uL of phenolphthalein indicator. Then, titration was performed using a 0.1 mol/L NaOH solution. The endpoint was reached when the solution turned a faint pink color that remained unchanged for 0.5 minutes, and the volume of NaOH solution used was recorded. Each experiment was repeated three times. Distilled water was used as a blank control, replacing the hydrolysate for titration.

4.2.4.5 pH

The pH of the hydrolysate was determined using a WD-35634-30 digital pH meter (Oakton Instruments, Vernon Hills, IL, USA).

4.2.5 Plant growth indicators (SPAD, height and weight)

The chlorophyll content indices were recorded by SPAD values which were measured by method described previously in 2020 (Cristina et al., 2020) with a portable chlorophyll meter (SPAD-502, Minolta Camera Co. Ltd., Japan). Three plants were selected randomly per treatment for measurement. After harvest, the edible parts of seven plants were immediately weighed to record the fresh weight using an electronic scale (B604C, BOMATA, Japan). Height was measured using a ruler.

4.2.6 Statistical analysis

The experimental data are presented as the mean ± standard error of three replicates. The figures were prepared using OriginPro 2021 software (OriginLab, Northampton, MA).

4.3 Results and disscussion

4.3.1 Analysis of ions in hydrolysate

The amount of metal ions in the hydrolysate obtained from SST of BWW is shown in Table 4.1. These metal ions are typically the main components of seawater. Overall, in the SST process with BWW, the reduction of metal ions in the hydrolysate is caused by the adsorption effect of BWW. In this process, BWW acts as a hydrothermal carbon and adsorbs the metal ions in seawater through adsorption. This process is equivalent to desalination of seawater. Generally, with an increase in treatment temperature, the amount of residual metal ions in the hydrolysate shows a trend of initially decreasing and then increasing, with the maximum value reached at $H_{170°C}$. For example, the minimum values of Mg, K, Mn, Zn, and Cu are all obtained at $H_{170°C}$. This is because the adsorption effect of BWW increases due to the destruction of the surface structure of BWW after high-temperature treatment, resulting in an increased specific surface area of BWW. However, with further temperature increase, excessive BWW is dissolved into the solution, leading to a

decrease in the adsorption sites. Additionally, BWW itself contains a certain amount of ionic components that dissolve into the solution after BWW decomposition, resulting in an increase in ion content at $H_{230°C}$. However, this situation does not always occur, and in some cases, the content of certain ions shows a continuous decrease, such as Ca, Ni, and Co.

Table 4.1 The content of metal ions in the hydrolysate (after drying).

	CK	$H_{110°C}$	$H_{170°C}$	$H_{230°C}$
TN (%)	0.06	0.44	0.41	0.90
N-NO3-(%)	0.00	1951.97	1701.22	1878.92
N-NH4+(%)	1646.34	965.07	1577.24	2457.40
P(%)	0.027	0.10	0.11	0.12
K(%)	1.11	2.61	2.39	2.64
Ca（%）	1.22	0.53	0.46	0.45
Mg（%）	3.73	3.17	2.81	3.36
Mn（ppm）	348.05	324.11	314.68	375.65
Zn（ppm）	170.02	150.85	145.09	199.43
Cu（ppm）	36.40	19.43	15.61	21.93
Ni（ppm）	78.90	43.89	42.03	37.22
Co（ppm）	285.73	200.66	201.87	189.64

The content of N, P and K is also shown in Table 4.1. The concentrations of total N, P, and K in the hydrolysate significantly increased after SST. The N, P, and K concentrations in seawater were only 0.06, 0.03, and 1.11, respectively. However, at $H_{230°C}$, they reached their maximum values of 0.90, 0.12, and 2.64, respectively. This is likely due to the dissolution of nitrogen from BWW into the hydrolysate after SST. N, P, and K are three essential nutrients for plant growth, each playing different roles and functions. N is a key component in the formation of proteins, nucleic acids, and amino acids in plant biomass (Stéphanie et al., 2009). It plays a crucial role in promoting plant growth rate and photosynthetic efficiency. P is a vital component of nucleic acids, ATP (adenosine triphosphate), phospholipids, etc., participating in crucial reactions related to energy transfer and storage (Eutropia et al., 2013). P is essential for root development, flower bud formation, and fruit development in plants. K plays an important role in regulating osmotic pressure, maintaining ion balance, and modulating enzyme activity within plant cells (Wahid et al., 2022). It significantly affects water regulation, photosynthesis, leaf morphology, and agricultural product

quality. These nutrients play distinct roles in plants, participating in various biochemical processes and significantly influencing plant morphology, physiology, and yield. SST facilitates the release of N, P and K elements from BWW into the hydrolysate, ensuring the supply of essential elements required by plants.

Table 4.2 EC, pH and volume of hydrolysate.

	Liquid			Solid
	EC	pH	Volume (mL)	Weight (g)
CK	21.06	7.23	150	6.00
$H_{110℃}$	22.10	4.29	106	5.35
$H_{170℃}$	22.22	3.44	105	4.25
$H_{230℃}$	22.28	3.29	116	3.11

Table 4.2 was the EC, pH and volume of hydrolysate. As we know, the electrical conductivity (EC) of seawater is already high, but after SST, the EC value becomes even higher. Through analysis of metal ions in the period section, it can be concluded that the increase in EC content is not due to the presence of metal ions. The increase in EC value may be related to the generation of acids, which undergo ionization and produce H^+. The increase in these ions at high temperatures leads to the elevation of EC value. The increase in acidity also results in a decrease in pH value. The original pH value of seawater is 7.23, whereas in the hydrolysis solution at $H_{230℃}$, the pH value is only 3.29. The volume of the hydrolysis solution has also been measured, with the addition of 150 units of seawater. After subcritical treatment, the volumes of the hydrolysis solution at $H_{110℃}$ and $H_{170℃}$ are 106 and 105, respectively, while at $H_{230℃}$, the volume is 116 mL. The obtained volume of the hydrolysis solution is less than the initially added amount due to the permeation and retention of some seawater in the SST process, likely caused by forces or chemical interactions. It is worth noting that from $H_{110℃}$ to $H_{170℃}$, the volume of the hydrolysis solution remains almost unchanged. However, when the temperature reaches $H_{230℃}$, the volume significantly increases. This may be due to a greater degradation of BWW at high temperatures, resulting in a decrease in the amount of solids and a reduction in the amount of liquid attached to the solids. The amounts of solids in each group also confirm this observation. It can be seen that as the temperature increases, the weight of residues decreases, reaching the minimum value (3.11g) at $H_{230℃}$. This also indicates that

BWW was effectively degraded under SST treatment, with a significant amount of components dissolved into the hydrolysate.

4.3.2 Analysis of organic components in hydrolysate

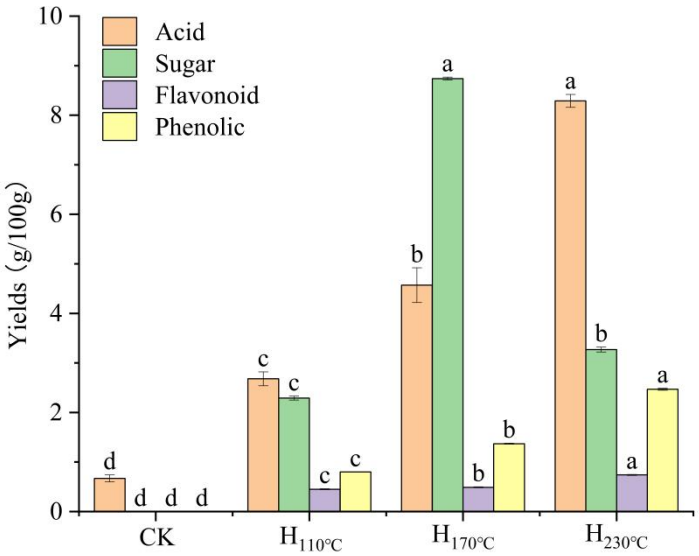

Figure 4.2 Organic components yiled in hydrolysate.

BWW undergoes SST under different temperature conditions, resulting in the degradation and dissolution of free components, generating organic compounds. These organic compounds typically include sugars, flavonoids, phenols, and acidic components (Yuan et al., 2023). Their contents have been detected and shown in Figure 4.2. Total phenols and total flavonoids in the hydrolysate originate from the degradation of lignin in BWW at high temperatures and the dissolution of free flavonoids and phenolic components. The contents of total phenols and total flavonoids increase with increasing temperature, reaching maximum values of 2.47 and 0.74 at $H_{230°C}$. This indicates that increasing temperature promotes the degradation of lignin in BWW and the dissolution of these bioactive substances in the hydrolysate. The reducing sugars in the hydrolysate result from the degradation of cellulose and hemicellulose, as well as the dissolution of polysaccharide components in BWW. The trend of reducing sugar content shows an initial increase followed by a decrease, with a maximum value of 8.74 at $H_{170°C}$, attributed to the degradation of sugars caused by high temperature. The content of acids in the hydrolysate also increases with increasing temperature, with a maximum value of 8.29 observed at

$H_{230°C}$. These acids may originate from the dissolution of volatile acids present in the BWW itself, as well as the acidic components produced from the degradation of sugars, as mentioned in Yuan et al (Yuan et al., 2022). Additionally, some phenolic components also contribute to the acidity.

4.3.3 The growth of lettuce under different liquid fertilizers varies.

Table 4.3 shows the average values of height and weight for lettuce. Both the height and weight of lettuce exhibit a trend of initially increasing and then decreasing, with the maximum values obtained at $H_{170°C}$. This indicates that compared to the control group (CK), the components extracted from the hydrolysate at this temperature and the residual ion content in the hydrolysate have a promoting effect on plant growth. However, higher temperatures may lead to the degradation of certain components, which are detrimental to plant growth and can even cause inhibition. The lower height and weight of the $H_{230°C}$ group compared to the CK group also confirm this result. These inhibitory components may inhibit plant growth by affecting the microorganisms in the soil or influencing the plant's ability to absorb water through its root system, among other factors.

Table 4.3 Average height and weight of lettuce. Average ± s.d. significant differences occur when the alphabets are different in a column ($P < 0.05$).

	Height (cm)	Weight (g)	SPAD
CK	14.93 ± 1.30^{a}	20.43 ± 2.40^{b}	25.01 ± 4.26^{b}
$H_{110°C}$	15.00 ± 1.66^{a}	22.96 ± 1.91^{a}	27.70 ± 3.85^{b}
$H_{170°C}$	15.14 ± 1.41^{a}	23.51 ± 1.53^{a}	26.61 ± 2.41^{b}
$H_{230°C}$	12.79 ± 1.52^{b}	18.31 ± 2.50^{b}	23.86 ± 2.95^{b}

SPAD is used to evaluate the chlorophyll content index. Chlorophyll is crucial for plants as it is a key pigment in photosynthesis, capable of absorbing light energy, converting it into chemical energy, and participating in organic compound synthesis. Chlorophyll also regulates light utilization, protects cells, and regulates growth and development, playing a significant role in plant life activities. The SPAD value for the control group was 25.01, with the highest value of 27.70 achieved at $H_{110°C}$. Subsequently, as the temperature increased, the chlorophyll content index showed a decreasing trend, being lower than the control group at $H_{230°C}$. This could be attributed to the degradation of new compounds in the SST hydrolysis solution at excessively

high temperatures, which inhibited chlorophyll synthesis. Alternatively, the presence of certain components may have caused an imbalance in nutrient concentration within the plant, thereby affecting chlorophyll synthesis and regulation, resulting in a decrease in SPAD values.

Figure 4.3 illustrates the growth of lettuce cultivated under different liquid fertilizers. It is evident that lettuce grown at $H_{110℃}$ and $H_{170℃}$ is larger than CK and $H_{230℃}$. The largest lettuce observed was obtained at $H_{170℃}$. The observed size of lettuce is consistent with the measured weight and height of the lettuce, indicating that the content of various components in the hydrolysis solution obtained from SST at 170 ℃ is more conducive to the growth of lettuce compared to seawater.

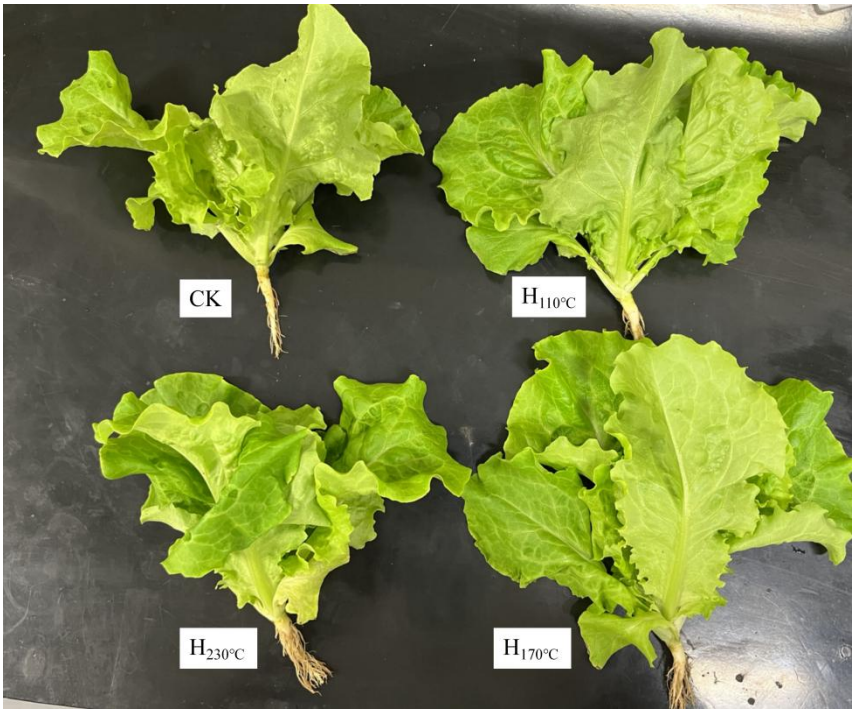

Figure 4.3 The growth of lettuce under different liquid fertilizers varies.

4.4 Conclusion

Compared to seawater, the application of subcritical seawater hydrolysate in lettuce cultivation has shown better results. The optimum value is achieved at $H_{170℃}$. Due to the adsorption effect of BWW, SST effectively reduces the concentration of ions in the hydrolysate. Organic substances in BWW, such as antioxidants, sugars, and proteins, dissolve into the hydrolysate. As a liquid fertilizer, the hydrolysate provides necessary nutrients to lettuce cultivation and alleviates salt stress. Various growth

parameters of lettuce were also measured, and lettuce grown with liquid fertilizer at $H_{170°C}$ exhibited the highest height and weight, measuring 15.14cm and 23.51g, respectively. This study not only demonstrates the application of desalinated seawater in cultivation but also facilitates the resource utilization of BWW. It provides a new avenue for the resource utilization of BWW, enabling further in-depth exploration to determine the optimal treatment conditions.

Chapter 5. Conclusion and recommendation

5.1 Conclusion

The subcritical liquid treatment method was used to treat BWW, including SWT and SEST. Pilot-scale verification was conducted, and ultimately, SST was applied to BWW treatment, with the hydrolysate used as liquid fertilizer in lettuce cultivation. The main focus was on different treatment temperatures as the key indicator, and the content of sugars, flavonoids, phenols, and other compounds in the liquid phase was measured. The content of cellulose, hemicellulose, lignin, and other components in the solid phase was also measured. Biomass conversion assessment was performed as well. Based on the reaction mechanism, physical properties, and application aspects of the BWW samples, the optimal pretreatment conditions were determined. Summarizing the research based on the above content, the experimental results are as follows:

(1) A higher sum of saccharides yields of 4.10 % was obtained at a relatively lower severity factor (SF) of 3.24 with a byproducts yield of 1.92 %. The contents of cellulose, hemicellulose, and lignin were analyzed in the residue after SWT. Enzymatic hydrolysis from the residue of SWT was inhibited. Thus, enzymatic hydrolysis for saccharides is not suitable for utilizing the residue after SWT of BWW. Meanwhile, the surface morphology and biomass conversion were analyzed in this study. These results demonstrate that the SWT process is efficient for treating BWW and producing saccharides. This work lays a foundation for the industrial application of BWW, and for improving the economic benefits of buckwheat cultivation.

(2) During the SEST, degradation of lignin and dissolution of extractives increased the total phenolics yield. The increase in the temperature led to the degradation of some flavonoid components. Reducing sugars were mainly present as polysaccharides because of the low extraction temperature. Water and ethanol exhibited synergistic effects under subcritical conditions, which resulted in degradation of more lignin and extraction of more bioactive components than hydrothermal extraction, while retaining cellulose and hemicellulose. In the pilot-scale experiment, the total yields of phenolics, flavonoids, and reducing sugars

were 29.8 ± 0.1, 13.9 ± 0.5, and 33.9 ± 0.5 g/kg, respectively. The turbidity and Brix values of the liquid samples obtained by SEST were high because of breakdown of the structure of the BWW and the dissolution of the bioactive components. Additionally, compared with the laboratory scale, better results were obtained on the pilot scale because of greater feedstock homogeneity and equipment parameters. SEST is a promising approach that could be used on the pilot scale to depolymerize BWW and extract bioactive components.

(3) The optimum value is achieved at 170 ℃. Due to the adsorption effect of BWW, SST effectively reduces the concentration of ions in the hydrolysate. Organic substances in BWW, such as antioxidants, sugars, and proteins, dissolve into the hydrolysate. As a liquid fertilizer, the hydrolysate provides necessary nutrients to lettuce cultivation and alleviates salt stress. Various growth parameters of lettuce were also measured, and lettuce grown with liquid fertilizer at 170 ℃ exhibited the highest height and weight, measuring 15.14cm and 23.51g, respectively. Hydrolysate also promotes the synthesis of chlorophyll. This study not only demonstrates the application of desalinated seawater in cultivation but also facilitates the resource utilization of BWW.

5.2 Recommendation

This study has provided valuable insights into the investigated subject. However, there are several avenues for further research that can contribute to a deeper understanding and advancement of the field. The following research recommendation highlights potential areas for future investigations:

(1) In the first part of the study, SWT was performed on BWW, and the content of monosaccharides obtained was not very high. A significant portion of sugars was found to exist in the form of polysaccharides. Therefore, future research should explore the use of environmentally friendly and non-polluting catalysts to promote sugar production. In the second part of the study, SEST was conducted on BWW, resulting in relatively low yields of bioactive substances. This could be attributed to the large size of BWW straw and the low processing temperature, which led to incomplete degradation and dissolution of the majority of components. Therefore,

further in-depth research is needed to improve the yield of bioactive substances.

(2) Although pilot-scale experiments were conducted in this study, it is important to note that scaling up the process may introduce new challenges, leading to discrepancies between the pilot-scale and laboratory-scale results. Therefore, more comprehensive exploratory research and analysis of the underlying reasons are required. Additionally, the quantity of bioactive compounds extracted in this study was limited, and the concentration was low. Hence, further research on purification processes is necessary. This would not only complement the current study but also promote the industrial application of extraction industry.

(3) In this study, SST was applied to BWW, and the hydrolysate was used as a liquid fertilizer for cultivation was an exploratory approach. However, several issues remain unresolved, such as determining the optimal temperature for SST, assessing the impact of excessive acid generated during degradation on plants, investigating the effect of solid-liquid ratio and ion adsorption from seawater, and exploring the limited growth-promoting effect of SST hydrolysate as a liquid fertilizer on lettuce. Subsequent research should focus on gradually optimizing these aspects.

(4) The entire study was based on the utilization of hydrolysate, which generates a substantial amount of residue. This residue represents an important waste resource that can be further utilized and recycled. Therefore, future research should investigate the resource utilization of residues to achieve biorefinery effects, ultimately aiming for zero waste.

Reference

Ahmad F, Silva EL, Varesche MBA. Hydrothermal processing of biomass for anaerobic digestion-A review. Renew. Sustain. Energy Rev. 2018, 98: 108-124.

Alonso-Riaño P, Ramos C, Trigueros E, Beltrán S, Sanz MT. Study of subcritical water scale-up from laboratory to pilot system for brewer's spent grain valorization. Ind. Crop Prod. 2023, 191: 115927.

Ana LH, Judit MJ, Silvia BR. Study of steam explosion pretreatment and preservation methods of commercial cellulose. Carbohyd. Polym. 2018, 191: 234-241.

Ando H, Sakaki T, Kokusho T, Shibata M, Uemura AY. Hatate Y. Decomposition behavior of plant biomass in hot-compressed water. Ind. Eng. Chem. Res. 2000, 39: 3688–3693.

Aydin A, Kant C, Turan M. Humic acid application alleviate salinity stress of bean (Phaseolus vulgaris L.) plants decreasing membrane leakage. Afr. J. Agr. Res. 2012, 7(7): 1073-1086.

Bahram F, Malihe A, Ali RB. Energy, environmental, and economic efficiency in fossil fuel exporting countries: A modified data envelopment analysis approach. Sustain. Prod. Consump. 2021, 26: 588-596.

Ballesteros I, Oliva JM, Negro MJ, Manzanares P, Ballesteros M. Enzymic Hydrolysis of Steam Exploded Herbaceous Agricultural Waste (Brassica carinata) at Different Particle Sizes. Process Biochem. 2002, 38(2):187-192.

Batista G, Souza RB, Pratto B, dos Santos-Rocha MS, Cruz AJ. Effect of severity factor on the hydrothermal pretreatment of sugarcane straw. Bioresour. Technol. 2018, 275: 321–327.

Bernhoft A. A brief review on bioactive compounds in plants. In: Proceedings from a symposium held at The Norwegian Academy of Science and Letters, Oslo, Norway. 2010.

Bonafaccia G, Marocchini M, Kreft I. Composition and technological properties of the flour and bran from common and tartary buckwheat. Food Chem. 2003, 80: 9-15.

Brand S, Hardi F, Kim J, Suh DJ. Effect of heating rate on biomass liquefaction:

differences between subcritical water and supercritical ethanol. Energy 2014, 68: 420-427.

Broekman S, Pohlmann O, Beardwood ES, de Meulenaer EC. Ultrasonic treatment for microbiological control of water systems. Ultrason. Sonochem. 2010, 17(6): 1041-1048.

Brunecky R, Vinzant TB, Porter SE, Donohoe BS, Johnson DK, Himmel ME. Redistribution of xylan in maize cell walls during dilute acid pretreatment. Biotechnol. Bioeng. 2008, 102: 1537-1543.

Chen JX, Wang X, Zhang BY, Yang YF, Song YB. Integrating enzymatic hydrolysis into subcritical water pretreatment optimization for bioethanol production from wheat straw. Sci. Total Environ. 2021, 770: 145321.

Cristina G, Camelin E, Tommasi T, Fino D, Pugliese M. Anaerobic digestates from sewage sludge used as fertilizer on a poor alkaline sandy soil and on a peat substrate: Effects on tomato plants growth and on soil properties. J. Environ. Manage. 2020, 269: 110767.

Croteau R, Kutchan TM, Lewis NG. Natural products (secondary metabolites). In: Buchanan B, Gruissem W, Jones R, (Eds.). Biochemistry and Molecular Biology of Plants. American Society of Plant Physiologists, Rockville, MD, 2000, 1250–1318.

Del Castillo-Llamosas A, Rodríguez-Martínez B, Pablo G, Eibes G, Garrote G, Gullón B. Hydrothermal treatment of avocado peel waste for the simultaneous recovery of oligosaccharides and antioxidant phenolics. Bioresour. Technol. 2021, 342: 125981.

Deng J, Jia G. Dielectric constant prediction of pure organic liquids and their mixtures with water based on interpretable machine learning. Fluid Phase Equilib. 2022, 561: 113545.

Dziedzic K, Górecka D, Szwengiel A, Sulewska H, Kreft I, Gujska E, Walkowiak J. The Content of Dietary Fibre and Polyphenols in Morphological Parts of Buckwheat (Fagopyrum tataricum). Plant Food Hum. Nutr. 2018, 73: 82-88.

Elliott DC, Biller P, Ross AB, Schmidt AJ, Jones SB. Hydrothermal liquefaction of

biomass: developments from batch to continuous process. Bioresour. Technol. 2015, 178: 147-156.

Elsayed M, Andres Y, Blel W, Hassan R, Ahmed, A. Effect of inoculum VS, organic loads and I/S on the biochemical methane potential of sludge, buckwheat husk and straw. Desalin. Water Treat. 2019, 157: 69-78.

Essien SO, Young B, Baroutian S. Recent advances in subcritical water and supercritical carbon dioxide extraction of bioactive compounds from plant materials. Trends Food Sci. Technol. 2020, 97: 156-169.

Faeth JL, Valdez PJ, Savage PE. Fast hydrothermal liquefaction of nannochloropsis sp to produce biocrude. Energ. Fuel 2013, 27(3): 1391-1398.

Fang C, Thomsen MH, Brudecki GP, Cybulska I, Frankær CG, Bastidas-Oyanedel JR, Schmidt JE. Seawater as Alternative to Freshwater in Pretreatment of Date Palm Residues for Bioethanol Production in Coastal and/or Arid Areas. ChemSusChem. 2015, 8(22): 3823-3831.

Farzaneh T, Lizbeth LP, Hasan A, Bruce ED. Optimization of the ammonia fiber explosion (AFEX) treatment parameters for enzymatic hydrolysis of corn stover. Bioresour. Technol. 2005, 96(18): 2014-2018.

Gao D, Kobayashi T, Adachi S. Kinetics of sucrose hydrolysis in a subcritical water-ethanol mixture. J. Appl. Glycosci. 2014, 61: 9-13.

Gao Y, Wang H, Guo J, Peng P, Zhai M, She D. Hydrothermal degradation of hemicelluloses from triploid poplar in hot compressed water at 180-340 °C. Polym. Degrad. Stab. 2016, 126: 179-187.

Germ M, Arvay J, Vollmannová A, Tóth T, Golob A, Luthar Z, Kreft I. The temperature threshold for the transformation of rutin to quercetin in Tartary buckwheat dough. Food Chem. 2019, 283: 28-31.

Gu X, Pang N, Qiu Y, Fu X, Yao Y, Chen S. Systematic evaluation of fractionation and valorization of lignocellulose via two-stage hydrothermal liquefaction. Fuel 2022, 310: 122358.

Haruna SA, Li H, Wei W, Geng W, Luo X, Zareef M, Adade SYSS, Ivane NM, Isa A, Chen Q. Simultaneous quantification of total flavonoids and phenolic content in

raw peanut seeds via NIR spectroscopy coupled with integrated algorithms. Spectroc. Acta Pt. A-Molec. BioMolec. Spectr. 2023, 285: 121854.

Hassan F, Al-Yasi H, Ali E, Alamer K, Hessini K, Attia H, El-Shazly S. Mitigation of salt-stress effects by moringa leaf extract or salicylic acid through motivating antioxidant machinery in damask rose. Can. J. Plant Sci. 2020, 101(2): 157-165.

Haverly, MR, Schulz TC, Whitmer LE, Friend AJ, Funkhouser JM, Smith RG, Young MK, Brown RC. Continuous solvent liquefaction of biomass in a hydrocarbon solvent. Fuel 2018, 211: 291-300.

Himmel ME, Picataggio SK. Our Challenge is to Acquire Deeper Understanding of Biomass Recalcitrance and Conversion. In Biomass Recalcitrance: Deconstructing the Plant Cell Wall for Bioenergy; Wiley-Blackwel: Chichester, UK, 2008, 1-6.

Holasova M, Fiedlerova V, Smrcinova H, Orsak M, Lachman J, Vavreinova S. Buckwheat—the source of antioxidant activity in functional foods. Food res. Int. 2002, 35: 207-211.

Hu X, Zhang G, Hamaker BR, Miao M. The contribution of intact structure and food processing to functionality of plant cell wall-derived dietary fiber, Food Hydrocoll. 2022, 127: 107511.

Huda MN, Lu S, Jahan T, Ding M, Jha R, Zhang K, Zhang W, Georgiev MI, Park SU, Zhou M. Treasure from garden: Bioactive compounds of buckwheat, Food Chemistry 2021, 335: 127653.

Ji XL, Han L, Liu F, Yin S, Peng Q, Wang M. A mini-review of isolation, chemical properties and bioactivities of polysaccharides from buckwheat (Fagopyrum Mill). Int. J. Bio. Macromol. 2019, 127: 204-209.

Jiang J, Peng Y, Ran Y, Cao J. Pseudo lignin formed from hygrothermally treated holocellulose and its effect on fungal degradation. Ind. Crop. Prod. 2022, 184: 115004.

Kalinová JP, Vrchotová N, Tříska J. Contribution to the study of rutin stability in the achenes of Tartary buckwheat (Fagopyrum tataricum). Food Chem. 2018, 258: 314-320.

Kellock M, Maaheimo H, Marjamaa K, Rahikainen J, Zhang H, Holopainen-Mantila U, Ralph J, Tamminen T, Felby C, Kruus K. Effect of hydrothermal pretreatment severity on lignin inhibition in enzymatic hydrolysis. Bioresour. Technol. 2019, 280: 303-312.

Khoulati A, Ouahhoud S, Mamri S, Alaoui K, Lahmass I, Choukri M, Saalaoui E. Saffron extract stimulates growth, improves the antioxidant components of Solanum lycopersicum L., and has an antifungal effect. Ann. Agr. Sci. 2019, 64(2): 138-150.

Kim DS, Kim MB, Lim SB. Enhancement of Phenolic Production and Antioxidant Activity from Buckwheat Leaves by Subcritical Water Extraction. Prev. Nutr. Food Sci. 2017, 22: 345-352.

Klinchongkon K, Chanthong N, Ruchain K, Khuwijitjaru P, Adachi S. Effect of ethanol addition on subcritical water extraction of pectic polysaccharides from passion fruit peel. J. Food Process. Preserv. 2017, 41: 13138.

Kraujalienė V, Pukalskas A, Venskutonis PR. Multi-stage recovery of phytochemicals from buckwheat (Fagopyrum esculentum Moench) flowers by supercritical fluid and pressurized liquid extraction methods. Ind. Crops Prod. 2017, 107: 271-280.

Levenda AM, Behrsin I, Disano F. Renewable energy for whom? A global systematic review of the environmental justice implications of renewable energy technologies. Energy Res. Soc. Sci. 2021, 71: 101837.

Li JJ, Zhang J, Zhang S, Gao Q, Li J. Alkali lignin depolymerization under eco-friendly and cost-effective NaOH/urea aqueous solution for fast curing bio-based phenolicresin. Ind. Crop. Prod. 2018, 120(1): 25-33.

Liu XX, Liu HM, Yan YY, Fan LY, Yang JN, Wang XD, Qin GY. Structural characterization and antioxidant activity of polysaccharides extracted from jujube using subcritical water. LWT-Food Sci. Technol. 2020, 117: 108645.

Lukšič L, Árvay J, Vollmannová A, Tomás T, Škrabanja V, Trček J, Germ M, Kreft I. Hydrothermal treatment of Tartary buckwheat grain hinders the transformation of rutin to quercetin. J. Cereal Sci. 2016, 72: 131-134.

Marianne Q, Jérôme H, Abdellatif B, Steyer JP, Carrère H, Trably E. Inhibition of

fermentative hydrogen production by lignocellulose-derived compounds in mixed culture. Int. J. Hydrogen Energ. 2012, 37(4): 3150-3159.

Meng X, Liu F, Xiao Y, Cao J, Wang M, Duan X. Alterations in physicochemical and functional properties of buckwheat straw insoluble dietary fiber by alkaline hydrogen peroxide treatment. Food Chem: X 2019, 3:100029.

Michaelides EE, Michaelides DN. Impact of nuclear energy on fossil fuel substitution. Nucl. Eng. Des. 2020, 366: 110742.

Milica N, Uroš G, Tomislav T, Nikola H, Nebojša N. Distribution of polyphenolic and sugar compounds in different buckwheat plant parts. RSC Adv. 2021, 11: 25816-25829.

Miller, GL. Use of Dinitrosalicylic Acid Reagent for Determination of Reducing Sugar. Anal. Chem. 1959, 31: 426-428.

Mohamad N, Abd-Talib N, Yong TLK. Furfural production from oil palm frond (OPF) under subcritical ethanol conditions. Mater. Today.: Proc. 2020, 31: 116-121.

Mohammadi HS, Asl AH, Khajenoori M. Determination of amiodarone hydrochloride solubility in pure and ethanol-modified subcritical water: experimental data and modeling. J. Mol. Liq. 2022, 362: 119679.

Mohammed, IS, Na RS, Kushima K, Shimizu N. Investigating the Effect of Processing Parameters on the Products of Hydrothermal Carbonization of Corn Stover. Sustainability 2020, 12: 5100.

Mohsen-Nia M, Amiri H, Jazi B, Dielectric constants of water, methanol, ethanol, butanol and acetone: measurement and computational study. J. Solut. Chem. 2010, 39: 701-708.

Mufari JR, Rodríguez-Ruiz AC, Bergesse AE, Miranda-Villa PP, Nepote V, Velez AR. Bioactive compounds extraction from malted quinoa using water-ethanol mixtures under subcritical conditions. LWT-Food Sci. Technol. 2021, 138: 110574.

Pena J, Villot A, Gerente C. Pyrolysis chars and physically activated carbons prepared from buckwheat husks for catalytic purification of syngas. Biomass Bioenerg. 2020, 132: 105435.

Pirzadah TB, Malik B, Kumar M, Rehman RU. Lignocellulosic Biomass: As Future Alternative for Bioethanol Production. Biomass Bioenerg. 2014, 46(39): 145-163.

Rajapaksha S, Shimizu N. Pilot-scale extraction of polyphenols from spent black tea by semi-continuous subcritical solvent extraction. Food Chem.: X 2022, 13: 100200.

Rajapaksha, S, Shimizu, N. Valorization of spent black tea by recovery of antioxidant polyphenolic compounds: Subcritical solvent extraction and microencapsulation. Food Sci. Nutr. 2020, 8: 4297-4307.

Ren, NQ, Zhao L, Chen C, Guo WQ, Cao GL. A review on bioconversion of lignocellulosic biomass to H_2: Key challenges and new insights. Bioresour. Technol. 2016, 215: 92-99.

Sabzoi N, Humair AB, Griffin GJ. An overview of effect of process parameters on hydrothermal carbonization of biomass. Renew. Sust. Energ. Rev. 2017, 73: 1289-1299.

Saha N, Saba A, Reza MT. Effect of hydrothermal carbonization temperature on pH, dissociation constants, and acidic functional groups on hydrochar from cellulose and wood. J. Anal. Appl. Pyrolysis 2019, 137: 138-145.

Sarker TR,Pattnaik F, Nanda S, Dalai AK, Meda V, Naik S. Hydrothermal pretreatment technologies for lignocellulosic biomass: A review of steam explosion and subcritical water hydrolysis. Chemosphere 2021,284: 131372.

Shao L, Chen H, Li Y, Li J, Chen G, Wang G. Pretreatment of corn stover via sodium hydroxide-urea solutions to improve the glucose yield. Bioresour Technol. 2020, 307: 123191.

Sharma V, Tsai ML, Nargotra P, Chen CW, Sun PP, Singhania RR, Patel AK, Dong CD. Journey of lignin from a roadblock to bridge for lignocellulose biorefineries: A comprehensive review. Sci. Total Environ. 2023, 861: 160560.

Shen N, Wang T, Gan Q, Liu S, Wang L, Jin B, Plant flavonoids: classification, distribution, biosynthesis, and antioxidant activity. Food Chem. 2022, 383: 132531.

Shen, XJ, Wang B, Huang PL, Wen JL, Sun RC. Effects of aluminum

chloride-catalyzed hydrothermal pretreatment on the structural characteristics of lignin and enzymatic hydrolysis. Bioresour. Technol. 2016, 206: 57-64.

Sluiter A, Hames B, Hyman D, Payne C, Ruiz R. Determination of Total Solids in Biomass and Total Dissolved Solids in Liquid Process Samples; National Renewable Energy Laboratory: Golden, CO, USA, 2008.

Sluiter A, Hames B, Ruiz R, Scarlata C, Sluiter J, Templeton D, Crocker D. Determination of Structural Carbohydrates and Lignin in Biomass; National Renewable Energy Laboratory: Golden, CO, USA, 2008.

Song X, Wachemo AC, Zhang L, Bai T, Li X, Zuo X, Yuan H. Effect of hydrothermal pretreatment severity on the pretreatment characteristics and anaerobic digestion performance of corn stover. Bioresour. Technol. 2019, 289: 121646.

Stéphanie M, Bernard, Habash, Dimah Z. The importance of cytosolic glutamine synthetase in nitrogen assimilation and recycling. New Phytologist 2009, 182: 608-620.

Suely A, Hossain MZ, Sahu JN, Chowdhury GF. Bioethanol production from water-soluble and structural carbohydrates of normal and high sugary corn stovers harvested at three growth stages. Energ. Convers. Manage. 2020, 221: 113104.

Sun Q, Chen WJ, Pang B, Sun Z, Lam SS, Sonne C, Yuan TQ. Ultrastructural change in lignocellulosic biomass during hydrothermal pretreatment. Bioresour. Technol. 2021, 341: 125807.

Tairo EV, Ndakidemi PA. Possible benefits of rhizobial inoculation and phosphorus supplementation on nutrition, growth and economic sustainability in grain legumes. Amer. J. Res. Communic. 2013, 1(12): 532-556.

Tang C, Shan J, Chen Y, Zhong L, Shen T, Zhu C, Ying H. Organic amine catalytic organosolv pretreatment of corn stover for enzymatic saccharification and high-quality lignin, Bioresour. Technol. 2017, 232: 222-228.

Tangkhavanich B, Kobayashi T, Adachi S. Effects of repeated treatment on the properties of rice stem extract using subcritical water, ethanol, and their mixture. J. Ind. Eng. Chem. 2014, 20: 2610-2614.

Tian CY, Li BM, Liu ZD, Zhang YH, Lu HF. Hydrothermal liquefaction for algal biorefinery: a critical review. Renew. Sustain. Energy Rev. 2014, 38: 933-950.

Toor SS, Rosendahl L, Rudolf A. Hydrothermal liquefaction of biomass: a review of subcritical water technologies. Energy 2011, 36 (5): 2328-2342.

Tran MQ, Nguyen VB, Duong KT, Le TML. The growth promotion effect of microelement fertilizers containing low molecular weight chitosan and xanthanon radish (Raphanus sativus L.). Nucl. Sci. Tech. 2020, 10(3): 22-30.

United Nations, Peace, dignity and equality on a healthy planet–Goal 7, 2016. https://unstats.un.org/sdgs/report/2016/goal-07/.

Vaickelionis G, VALANČIENĖ V. Lightweight concrete with an agricultural waste–buckwheat husk. Mater. Sci. 2016, 22(1): 98-104.

Wahid I, Rani P, Kumari S, Ahmad R, Hussain SJ, Alamri S, Khan MIR. Biosynthesized gold nanoparticles maintained nitrogen metabolism, nitric oxide synthesis, ions balance, and stabilizes the defense systems to improve salt stress tolerance in wheat. Chemosphere 2022, 287: 132142.

Wang QW, Su B, Zhou P, Chiu CR. Measuring total-factor CO_2 emission performance and technology gaps using a non-radial directional distance function: a modified approach. Energ. Econ. 2016, 56: 475-482.

Wikipedia, Water. https://en.wikipedia.org/wiki/Water.

Wikipedia, Ethanol. https://en.wikipedia.org/wiki/Ethanol.

Wu XF, Yin SS, Zhou Q, Li MF, Peng F, Xiao X. Subcritical liquefaction of lignocellulose for the production of bio-oils in ethanol/water system, Renew. Energy 2019, 136: 865-872.

Wu ZX, Wang J, Liu YJ, Hou SH, Liu XJ, Zhang Q, Cao F. A review of spectral controlling for renewable energy harvesting and conserving. Mat. Today Phys. 2021, 18: 100388.

Wu Z, Peng K, Zhang Y, Wang M, Yong C, Chen L, Qu P, Huang H, Sun E, Pan M, Lignocellulose dissociation with biological pretreatment towards the biochemical platform: a review. Mater. Today Bio 2022, 16: 100445.

Xiao X, Bian J, Li MF, Xu H, Xiao B, Sun RC. Enhanced enzymatic hydrolysis of

bamboo (Dendrocalamus giganteus Munro) culm by hydrothermal pretreatment. Bioresour. Technol. 2014, 159: 41-47.

Xu C, Liu F, Alam A, Chen H, Zhang Y, Liang C, Xu H, Huang S, Xu, J, Wang Z. Comparative study on the properties of lignin isolated from different pretreated sugarcane bagasse and its inhibitory effects on enzymatic hydrolysis. Int. J. Biol. Macromol. 2020, 146: 132-140.

Xu J, Xu LL, Zhou QW, Hao SX, Zhou T, Xie HJ. Enhanced in vitro antioxidant activity of polysaccharides from Enteromorpha prolifera by enzymatic degradation. J. Food Biochem. 2016 40: 275-283.

Yang J, Chen H, Liu Q, Zhou N, Wu Y, He Q. Is it feasible to replace freshwater by seawater in hydrothermal liquefaction of biomass for biocrude production? Fuel 2020, 282: 118870.

Yuan Y, Li F, Han N, Zeng B, Imaizumi Y, Na R, Shimizu, N. Exploring the Valorization of Buckwheat Waste: A Two-Stage Thermo-Chemical Process for the Production of Saccharides and Biochar. Fermentation, 2022,8(11): 573.

Yuan Y, Shimizu N, Li F, Magaña J, Li X. Buckwheat waste depolymerization using a subcritical ethanol solution for extraction of bioactive components: from the laboratory to pilot scale. J. Environ. Chem. Eng. 2023, 11(3): 109807.

Yuan Y, Xu X, Jing C, Zou P, Zhang C, Li Y. Microwave assisted hydrothermal extraction of polysaccharides from Ulva prolifera: functional properties and bioactivities. Carbohydr. Polym. 2018, 181: 902-910.

Yuan Z, Cheng S, Leitch M, Xu CC. Hydrolytic degradation of alkaline lignin in hot-compressed water and ethanol. Bioresour. Technol. 2010, 101: 9308-9313.

Zemnukhova LA, Tomshich SV, Shkorina ED, Klykov AG. Polysaccharides from buckwheat production wastes. Russ. J. Appl. Chem. 2004, 77: 1178-1181.

Zeng BY, Shimizu N. Hydrogen Generation from Wood Chip and Biochar by Combined Continuous Pyrolysis and Hydrothermal Gasification. Energies 2021, 14: 3793.

Zhang H, Han L, Dong H. An insight to pretreatment, enzyme adsorption and enzymatic hydrolysis of lignocellulosic biomass: Experimental and modeling

studies. Renew. Sustain. Energy Rev. 2021, 140: 110758.

Zhang R, Gao H, Wang Y, He B, Lu J, Zhu W, Peng L, Wang Y. Challenges and perspectives of green-like lignocellulose pretreatments selectable for low-cost biofuels and high-value bioproduction. Bioresour. Technol. 2023, 369: 128315.

Zhang X, Zhang W, Lei F, Yang S, Jiang J. Coproduction of xylooligosaccharides and fermentable sugars from sugarcane bagasse by seawater hydrothermal pretreatment. Bioresource Technology 2020, 309: 123385.

Zhao B, Wang H, Xu S, Qian L, Li H, Gao J, Zhao G, Ray MB, Xu CC. Influence of extraction solvents on the recovery yields and properties of bio-oils from woody biomass liquefaction in sub-critical water, ethanol or water–ethanol mixed solvent, Fuel 2022, 307: 121930.

Zheng Q, Li Z, Watanabe M. Production of solid fuels by hydrothermal treatment of wastes of biomass, plastic, and biomass/plastic mixtures: a review. J. Bioresour. Bioprod. 2022, 7: 221-244.

Zhou T, Jhamb S, Liang X, Sundmacher K, Gani R. Prediction of acid dissociation constants of organic compounds using group contribution methods. Chem. Eng. Sci. 2018, 183: 95-105.

Zhou Z, Liu D, Zhao X. Conversion of lignocellulose to biofuels and chemicals via sugar platform: an updated review on chemistry and mechanisms of acid hydrolysis of lignocellulose. Renew. Sustain. Energy Rev. 2021, 146: 111169.

Zhu YH, Biddy MJ, Jones SB, Elliott DC, Schmidt AJ. Techno-economic analysis of liquid fuel production from woody biomass via hydrothermal liquefaction (HTL) and upgrading, Appl. Energy. 2014, 129: 384-394.